2019

Soil moisture influences on radon fluxes in the Sydney Basin

Nicholas L. Keatley

Soil moisture influences on radon fluxes in the Sydney Basin

Abstract

Radon-222 is increasingly being used in air quality models as a tracer for understanding atmospheric dynamics and transport to improve the simulation of other key trace species such as CO2, CH4, NOx and O3. Applications such as this have driven efforts to improve the accuracy of radon emissions (also referred to as fluxes) in these models. Soil moisture is one of the primary factors which drives variations in radon emissions, and hence the concentration of radon in the atmosphere, however our understanding of the degree of its influence is currently lacking. This study aimed to gain a greater understanding of the influence of soil moisture on radon-222 emissions in the Sydney Basin over the period from January to December 2016. The focus of these efforts was aimed at determining the extent to which complexity of modelled soil moisture data influences the accuracy of modelled radon concentrations. This was done by comparing modelled radon concentrations derived from 4 distinct radon emissions maps with increasing levels of soil moisture complexity across varied climatic conditions and in response to a major rainfall event.

All modelled radon concentrations differed from observed values, with the best agreement shown by the most complex 'daily' emissions scenario with a correlation co-efficient of 0.68 for the whole year. In all instances, the two time-dependent, soil moisture driven scenarios performed very similarly to each other and exhibited greater precision than the two non-time-dependent scenarios, despite underestimating concentrations. A distinct diurnal cycle was observed for all scenarios, with peaks in night-time radon concentrations being poorly reflected by all of emissions scenarios, likely due to poor simulation of the nocturnal boundary layer. Following rainfall events all modelled radon concentrations more accurately reflected these observed night-time values. Both time-dependent scenarios exhibited decreased in emissions following rainfall, however the normalised mean bias remained relatively consistent throughout. This reflects the effective response of these more complex soil moisture driven, time-dependent scenarios, despite their underestimation of concentrations.

It is clear that implementing emissions estimates based on complex time-varying soil moisture inputs provides some improvement over more simple non-time varying methods. It is likely that further increasing complexity of the soil moisture models would provide little improvement for modelled radon concentrations. Rather improvements in the model itself, particularly its estimation of the nocturnal boundary layer, would assist in improving the accuracy of modelled radon concentrations. Thus, making radon a powerful diagnostic of model mixing and transport, in spite of the temporal variations in surface emissions.

Degree Type

Thesis

Degree Name

BEnviSci Hons

Department

School of Earth, Atmospheric & Life Sciences

Advisor(s)

Stephen Wilson

Keywords

Atmospheric modelling, emissions

Soil moisture influences on radon fluxes in the Sydney Basin

Nicholas Leo Keatley

Radon detector set up at Richmond study site (Photo Credit: ANSTO)

A thesis submitted in part fulfilment of the requirements of the

Bachelor of Environmental Science (Honours)

in the School of Earth, Atmospheric and Life Sciences,

Faculty of Science, Medicine and Health,

University of Wollongong 2019

November 2019

The information in this thesis is entirely the result of investigations conducted by the author, unless otherwise acknowledged, and has not been submitted in part, or otherwise, for any other degree or qualification.

Nicholas Leo Keatley

5th November 2019

Acknowledgements

- Dr Stephen Wilson and Dr Clare Murphy (University of Wollongong)
- Dr Alan Griffiths and Dr Alastair Williams (ANSTO)
- Melissa Booth

Abstract

Radon-222 is increasingly being used in air quality models as a tracer for understanding atmospheric dynamics and transport to improve the simulation of other key trace species such as CO_2, CH_4, NO_x and O_3. Applications such as this have driven efforts to improve the accuracy of radon emissions (also referred to as fluxes) in these models. Soil moisture is one of the primary factors which drives variations in radon emissions, and hence the concentration of radon in the atmosphere, however our understanding of the degree of its influence is currently lacking. This study aimed to gain a greater understanding of the influence of soil moisture on radon-222 emissions in the Sydney Basin over the period from January to December 2016. The focus of these efforts was aimed at determining the extent to which complexity of modelled soil moisture data influences the accuracy of modelled radon concentrations. This was done by comparing modelled radon concentrations derived from 4 distinct radon emissions maps with increasing levels of soil moisture complexity across varied climatic conditions and in response to a major rainfall event.

All modelled radon concentrations differed from observed values, with the best agreement shown by the most complex 'daily' emissions scenario with a correlation co-efficient of 0.68 for the whole year. In all instances, the two time-dependent, soil moisture driven scenarios performed very similarly to each other and exhibited greater precision than the two non-time-dependent scenarios, despite underestimating concentrations. A distinct diurnal cycle was observed for all scenarios, with peaks in night-time radon concentrations being poorly reflected by all of emissions scenarios, likely due to poor simulation of the nocturnal boundary layer. Following rainfall events all modelled radon concentrations more accurately reflected these observed night-time values. Both time-dependent scenarios exhibited decreased in emissions following rainfall, however the normalised mean bias remained relatively consistent throughout. This reflects the effective response of these more complex soil moisture driven, time-dependent scenarios, despite their underestimation of concentrations.

It is clear that implementing emissions estimates based on complex time-varying soil moisture inputs provides some improvement over more simple non-time varying methods. It is likely that further increasing complexity of the soil moisture models would provide little improvement for modelled radon concentrations. Rather improvements in the model itself, particularly its estimation of the nocturnal boundary layer, would assist in improving the accuracy of modelled radon concentrations. Thus, making radon a powerful diagnostic of model mixing and transport, in spite of the temporal variations in surface emissions.

Table of Contents

List of Figures

List of Tables

1. Introduction

In response to the growing industrialisation and the boom of large cities, it is necessary to understand the pollutants that are being emitted, their transport within the atmosphere, and ultimately their influence on the populations. These trace pollutants such as CO, O_3 and NO_x are emitted from various sources such as bushfires, photochemical smog, vehicle emissions and house - hold heating. All these source culminate to have a large and constantly changing influence on air quality and understanding these changes allow for appropriate management and planning to help minimise or negative effects of these pollutants. The Sydney Basin, encompassing Sydney and its surrounding suburbs, is prone to all these pollutants and emitting processes. Due to its dense population and being encompassed by a large escarpment, pollutants are prone to being trapped and can build up more so than other areas.

One very powerful tool for understanding these patterns is radon-222. It is a radioactive gas emitted from the earth and due to its properties similar to these trace gases and its stability as a noble gas (Sportisse, 2009), atmospheric radon can be used as a tracer for other atmospheric pollutants.

In order to use radon as a tracer, it must be first accurately modelled and simulated using chemical transport models and know radon emissions (Zahorowski et al., 2004).

As part of this it is important to determine the influence of soil moisture on these emissions and the degree to which soil moisture must be considered when modelling radon. Gaining a deeper understanding of this impact has the potential to improve simulated radon and in-turn be able to more effectively simulate the functioning of trace species.

1.1. Aims and Objectives

The aim of this study is to determine if the model error, in simulations of radon-222 in an air quality model, can be reduced by taking into account the effect of soil moisture on radon emissions, specifically within the Sydney Basin.

The primary objectives of this project are:

1. Examine trends of radon observation over time in relation to soil moisture.

2. Compare and evaluate model performance with radon flux parameterisations of varying complexities.
3. Investigate the sensitivity of emissions scenarios to varying atmospheric conditions.
4. Determine if the use of more sophisticated radon emissions maps leads to improved radon concentration.

1.2. Outline and Scope

This thesis will consist of five primary sections:

- Chapter 2: A literature review was undertaken presenting past research into atmospheric radon, its applications, its limitations and previous efforts that have attempted to gain a more complex understanding of surface radon emissions and their driving factors.
- Chapter 3: An outline of the study area and the dynamics of the Sydney basin that influence radon emissions and atmospheric concentrations, as well as a description of the focus study site at Richmond.
- Chapter 4: This chapter details the methods undertaken to complete the collection of the data used and the data analysis process.
- Chapter 5: A presentation and discussion of the results of the study through timeseries, diurnal cycles, scatter plots, normalised mean bias and emissions and concentrations maps.
- Chapter 6: A concise conclusion of the overall findings of the study and recommendations for future developments and research regarding radon emissions and soil moisture.

2. Literature Review

2.1. Radon: an overview

Radon-222 is a naturally occurring radioactive noble gas formed by the radioactive decay of radium-226, which is a member of the uranium-238 decay series. Uranium-238 is a primordial isotope which was present during the formation of the planet and this is naturally occurring within all soil and rocks around on Earth. However, the amount of uranium-238 present varies greatly dependent on the location of the source material, leading to large variations in radon emissions globally (Appleton, 2007).

Radon has a half-life of 3.8 days and undergoes decay within the atmosphere to form to form several metallic decay products, culminating in stable lead-206, as shown in Figure 1.This half-life is comparable to the lifetime of several other atmospheric pollutants such as CO, O_3 and NO_x (Sportisse, 2009) as well as the timescale of many other atmospheric dynamics, making it useful for comparing to these pollutants and atmospheric processes. Also, while it is radioactive and decay is its primary source of loss, radon is a noble gas, making it chemically stable and therefore a well-behaved passive tracer.

These factors all culminate to make studying radon a powerful method for understanding changes in emissions and transport schemes in atmospheric models (Zahorowski et al., 2004).

2.2. Motivation for studying atmospheric radon

The study of radon-222 (^{222}Rn) emissions from soil is a field that has developed immensely over the past 60 years due to the value of atmospheric radon as a diagnostic tool in atmospheric modelling. It is necessary to understand these emissions in depth in order to effectively simulate atmospheric radon concentrations. Otherwise, interest in radon has been driven by the need to manage the impacts of exposure to high radon levels on human health.

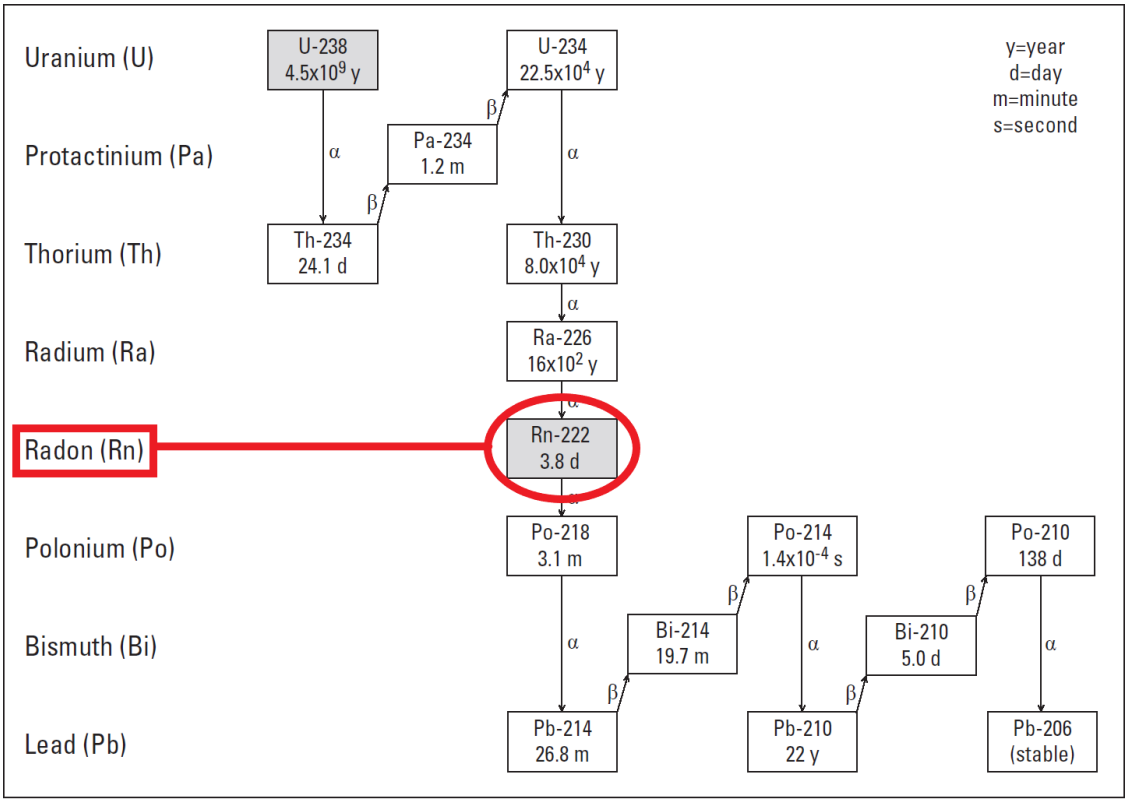

Figure 1: Radon-222 Decay series diagram (adapted from *Ayotte et al., (2007)).*

2.2.1. Human health concerns

Initial interest in radon came about due to numerous adverse health effects being noticed among miners as early as the 15th century (Vogiannis & Nikolopoulos, 2015). Many workers were found to have developed lung cancer at rates much higher than normal with a large amount of fatalities reported. The National Research Council, (1999) conducted an in-depth study of 60 000 miners over 50 years that found significantly higher rates of lung cancer amongst those working in mines than expected. Thus, the main locations in which radon has the potential to become a health risk is in environments underground such as mines or enclosed environments on the surface such as residential housing. This is due to the ability for radon levels to build up without adequate dispersion potential (Porstendörfer, 1994). The inhalation of these decay products is the primary source of health risk within these environments and is currently one of the two leading causes of lung cancer (Nazaroff & Nero, 1988; Yoon et al., 2016). Recent years have seen a decline in the focus on radon studies for human health, primarily as a result of decreasing public interest and education on the issue (Vogeltanz-Holm & Schwartz, 2018). Despite this, studying radon to understand its impact of human health is necessary, especially in regions such as North America and Europe which have been prone to high numbers of radon related lung cancer deaths (Field et al., 2006).

2.2.2. Atmospheric radon

The in-depth research in radon, motivated by its potential human health impacts, has provided a foundation of knowledge enabling the use of radon as a tracer in atmospheric studies. Atmospheric radon levels differ greatly to indoor levels and are an order of magnitude lower, thus posing no health risk to humans. However, the properties of atmospheric radon, as outlined in Section 2.1, and the role it plays in the atmosphere relative to other important pollutants provides its immense value for atmospheric studies (Zahorowski et al., 2004). Three of the primary purposes for studying atmospheric radon fluxes are; using radon as an atmospheric tracer for vertical mixing (Chambers et al., 2011), validation of chemical transport models (Chambers et al., 2019), and making regional flux estimates (Biraud et al., 2000). The resulting value of these studies comes in the form of a much deeper understanding of how atmospheric pollutants, especially those created by anthropogenic processes, are mixed and transported. This has been used in practice to study the human impact on

atmospheric pollutant levels as a result of land-use and activity changes such as traffic congestion (Williams et al., 2016) and population increases in urban areas (Chambers et al., 2015).

2.2.3. Observed radon as an atmospheric tracer

One of the primary uses for radon in atmospheric studies is as a tracer for vertical mixing processes. When studying radon the most powerful insights come from studying other trace species such as CO_2, CH_4, NO_x, O_3 etc. as these change over time and continue to impact the global climate (Zahorowski et al., 2004). Thus, further endeavours to gain a greater understanding of its functioning will increase its effectiveness as an atmospheric tracer and provide more insight into the functioning of atmospheric pollutants, specifically in urban areas.

The earliest interest radon as an atmospheric tracer began in 1928 with an attempt by Wigand and Wenk, (1928) to quantify lower atmosphere vertical mixing. This progressed further during the 1970's as Prospero and Carlson, (1970) found radon to be useful as a tracer for aerosol events. A further advancement came in the 1990's with the construction of direct radon monitors and its potential as a tracer in circulation models being realised (Zahorowski et al., 2004). More recent studies have focused on the use of radon as a tracer for understanding CO_2 fluxes. Hirsch, (2007) demonstrates how radon can be implemented to calculate regional scale CO_2 fluxes and in-turn allows for a greater understanding of the impact of industrial process on the amount of CO_2 being released into the atmosphere.

Understanding boundary layer properties and variations is another key parameter in effectively modelling atmospheric transport processes (Arya, 1999). Surface radon measurements can be used alongside other measurements such as lidar to be able to accurately constrain these changes in boundary layer mixing height (Griffiths et al., 2013). Understanding these variations in atmospheric structure can then be applied to modelling the distribution of pollutants and ozone in the atmosphere (Sesana et al., 1998; Williams et al., 2016).

2.2.4. Radon as an atmospheric tracer for model validation

Model validation represents a quantitative application of radon-222. As with the studies described above, radon acts as an atmospheric tracer, but here the radon fluxes are estimated and used as a

surface boundary condition in atmospheric chemistry and transport models (CTMs)(Griffiths et al., 2010; Karstens et al., 2015). This validation involves using the comparison of modelled radon vs observed radon values to assess the accuracy of modelled atmospheric processes and vertical mixing (Stockwell & Chipperfield, 1999). However, in order to effectively undertake this validation, reliable and widespread radon observation data must be available to compare against and incorporate into these models. Prior to the development of these radon flux maps, the most commonly method of modelling radon fluxes involved assuming a 1 atom cm^{-2} s^{-1} (~21 mBq m^{-2} s^{-1}) radon exhalation rate (Jacob & Prather, 1990) for all areas on land. This is due to the lack of widespread and long-running radon observations for many of the areas of study. This method, however, has some limitations in its application as it oversimplifies the spatial variation in radon fluxes due to a number of factors such as soil properties, radon abundance, topography and soil moisture. Despite these drawbacks, this method has proven to be effective due to the ubiquitous global presence of radon emissions from soil, the relatively uniform distribution of radium-226, and the relatively large errors that are present in the mixing and transport of radon in global CTM's (Gupta et al., 2004).Thus, as the representation of mixing and transport by these models improves, so does the need for radon emissions maps such as those developed by Griffiths et al., (2010) and Karstens et al., (2015). As these model's progress there is an ongoing challenge to improve these estimates so that they remain useful for model validation moving forward, as well as determining if these estimates are good enough or if they are overly complex.

2.2.5. Regional flux estimates of trace species

Due to its unique properties and ability to be used as an atmospheric tracer, radon can also be used to estimate fluxes of high interest greenhouse gases such as CO_2 (Hirsch, 2007). When using this approach, the area average radon flux is taken to be known, and atmospheric observations of radon and the species of interest are made simultaneously. Because both tracers are transported and mixed identically, the surface flux of the species of interest, upwind of the measurement station, can then be related to the ratio of the observed concentrations and the radon emission flux. Biraud et al., (2000) used this method when estimating European greenhouse gas emissions, specifically for understanding the emissions of unknown compounds in a variety of different atmospheric conditions.

The improvement and continued development of radon emissions maps will prove beneficial for all the atmospheric studies mentioned above, with varying degrees of impact. Specifically, the most significant impacts resulting from further improvements in radon emissions maps are the reduced uncertainty in regional flux estimates, as well as improved validation of atmospheric models.

2.3. Radon diffusion through soil

When considering the exhalation of radon-222, generated by decay of radioactive radium-226 in soil, there are a number of factors that influence the quantity and rate of radon being emitted from the soil. The three stages of radon transport through soil as shown in Figure 2 are: emanation from the source material, transport through soil layers, and exhalation from the soil into the atmosphere. It is necessary to consider all these factors when developing estimates of radon emissions in order to predict changes in emissions over space and time. For the purposes of this project, this process is being treated as one-dimensional steady state diffusion, based on Fick's Law ((Nazaroff, 1992)).

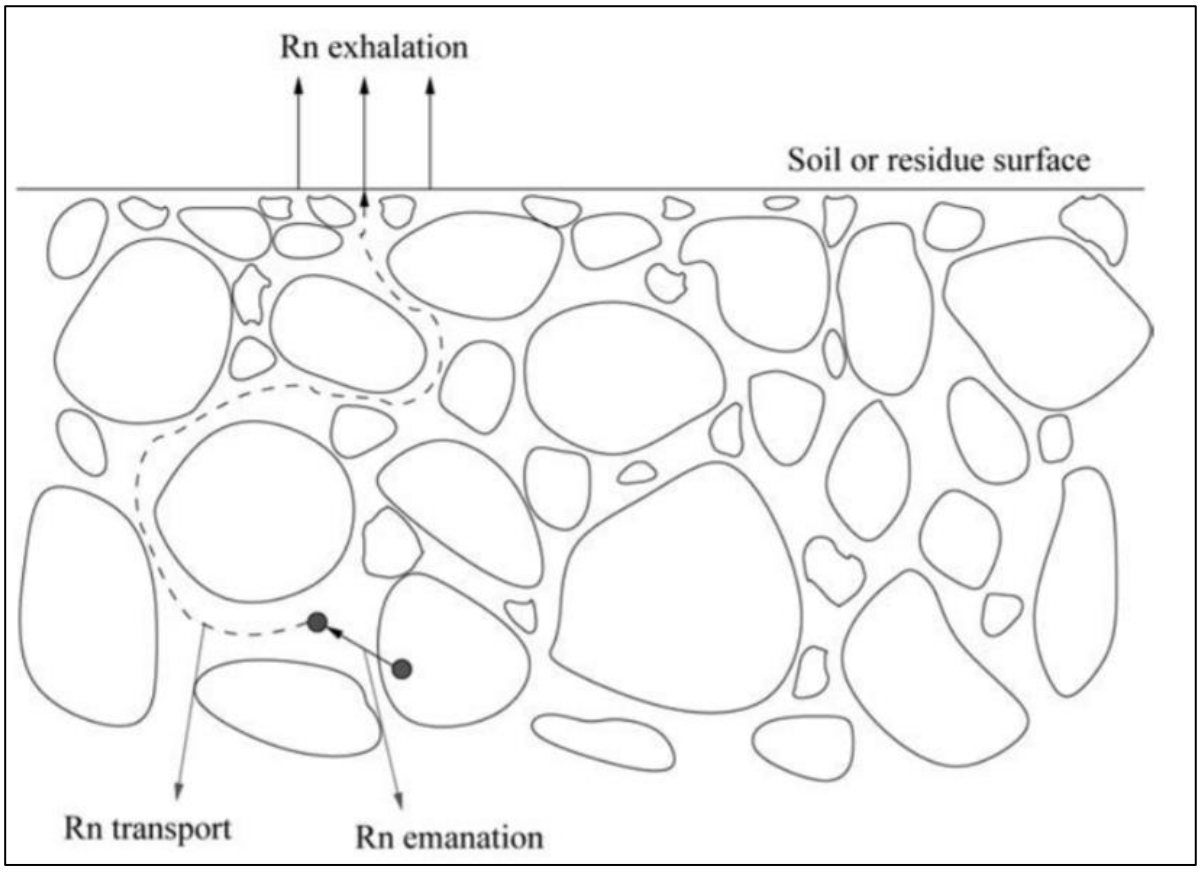

Figure 2: Process diagram of radon diffusion through soil (adapted from Ishimori et al., (2013)).

Thus, when considering only steady-steady state diffusive transport of radon from soil to air, the factors influencing diffusion are:

- Radium-226 content in soil
- Soil properties, e.g. grain size, porosity, emanation fraction etc.
- Effective diffusivity of soil, driven by soil moisture and temperature.

Diffusion can be calculated by incorporating these factors, using the equation for calculating surface

$$J(0) = -\rho_b A_{Ra} \int \sqrt{D_e}$$

flux density, $J(0)$, from Griffiths et al., (2010),

with the following parameters,

- ρ_b = dry soil bulk density.
- A_{Ra} = specific activity of radium-226 (units of activity per mass of dry soil).
- $\int$ = emanation factor.
- D_e = effective diffusivity (which accounts for soil moisture and temperature).

These parameters all influence the surface flux density of radon; however, soil moisture is the parameter which varies significantly with time and has the potential to cause temporal variations in the surface radon flux. Temperature also varies with time; however, these variations aren't significant at depth and diffusion is significantly less sensitive to diffusion than it is to soil moisture.

This is the primary justification for focusing on soil moisture and seeking to gain a deeper understanding of its influence on radon emissions. Better soil moisture estimates have the potential to bring improved estimation of temporal changes within these radon flux maps.

2.4. Soil moisture parameterization techniques

As noted above, soil moisture is one of the key driving factors influencing radon emissions from soil. The reason that soil moisture is a particularly influential characteristic is that it plays a direct role in physically limiting the diffusion of radon through soil (Griffiths et al., 2010; Nazaroff, 1992). Seasonal variations in radon emissions are also heavily influenced by soil moisture levels as they correspond with changes in weather patterns (Griffiths et al., 2010).

The limiting factors that have the potential to influence soil moisture estimates are sources of soil moisture data as well as the method used to parameterize its impact on diffusion.

There are two primary soil moisture parameterization methods which attempt to quantify the diffusion of radon through moist soil. These were formulated by Millington and Quirk, (1960) and Rogers and Nielson, (1991). These act as the basis for modern day models which include soil moisture as an input and there is some contention of which measure of effective diffusivity (D_e) should be used in radon flux maps (Griffiths et al., 2010; Karstens et al., 2015).

2.4.1. Millington & Quirk

This parameterization is one of the earlier soil moisture diffusion models created requiring soil moisture and porosity as inputs (Millington & Quirk, 1960). The initial experimental basis for this method is from Taylor, (1949) which is based on oxygen diffusion through soil.

This method defines effective diffusivity based on comparisons with these experimental results testing change in gas diffusion through soil with increasing soil moisture (Millington & Quirk, 1960).

$$D_e = D_{a0} \left(\frac{\epsilon - m^2}{\epsilon^{\frac{2}{3}}} \right)$$

The effective diffusivity (D_e) is calculated using,

with the following parameters:

- D_{a0} = Diffusion co-efficient for radon in air = 1.1x10^{-5} m^2 s^{-1}.
- ε = porosity.
- m = moisture saturation ($0 \leq m \leq 1$).

Karstens et al., (2015) implemented this parameterization in their radon flux map for Europe and argued for its effectiveness over the Rogers and Nielson, (1991) parameterization. Jin and Jury, (1996) have found it to strongly agree with large datasets of observational data when the two are compared. Karstens et al., (2015) also shows that it produces similar results to the newer more complex model by Moldrup et al., (2004), and recommend its use in the production of large-scale radon emissions maps.

2.4.2. Rogers and Neilson

This parameterization is a more recent development however it adopts the same inputs of soil moisture and porosity as the Millington and Quirk, (1960) model. The initial parametrization data for this model is derived from early US government laboratory tests in response to human health concerns (Kalwarf et al., 1982; Nielson et al., 1981).

This method defines the effective diffusivity based on observed correlations between radon diffusion and soil moisture (Rogers & Nielson, 1991). This effective diffusivity (D_e) is calculated using the equation,

$$D_e = D_{a0}\,\epsilon \exp(-6m\epsilon - 6m^{14\epsilon})$$

with the following parameters:

- D_{a0} = Diffusion co-efficient for radon in air = 1.1x10^{-5} m^2 s^{-1}.
- ε = porosity.
- m = moisture saturation ($0 \leq m \leq 1$).

This model is adopted in several studies that have produced radon flux estimates (Griffiths et al., 2010; Zhuo et al., 2008). Due to its differences in initial parameterization method, Karstens et al.,

(2015) found this model to underestimate measured diffusivity, leading to potential inaccuracies in its estimates.

Both models can also incorporate the dependence of diffusivity on temperature as determined by (Schery & Wasiolek, 1998) using the equation,

$$D_e(T) = D_e \left(\frac{T}{273}\right)^{\frac{3}{2}}$$

In practice, both soil moisture parameterization methods have been used to effectively reproduce soil moisture effects, resulting in regional scale radon flux estimates (Karstens et al., 2015). The current limiting factor to the spatial and temporal aspect of these soil moisture parameterizations is the availability of high-resolution soil moisture input data on a continental scale. This leads to reduced accuracy of spatial and temporal variations in soil moisture and resulting radon flux estimates.

Currently, these radon flux maps rely on modelled soil moisture datasets such as AWRA-L (Frost, 2018) and GLDAS Noah (Rodell et al., 2004)to provide a spatially complete input of soil moisture, primarily due to the lack of direct soil moisture measurements on a continental scale. Thus, as the availability of input data increases and the ability of these models to accurately estimate soil moisture improves, so will the ability of these radon flux maps to effectively estimate spatial and temporal variations in radon diffusion through soil.

While they are shown to be effective on the scale of individual sites, these models are limited by their requirement for comprehensive soil moisture and soil porosity data which prevents them from being used on a continental scale.

2.4.3. Limitations of steady state diffusive transport models

One of the major limitations of steady state diffusive transport models is that they overlook one of the primary drivers of radon emissions, advective transport. Currently, these radon flux maps are based on steady-state diffusive transport models, which on their own fail to consider advective transport of radon through soil, which is a large factor in influencing radon fluxes (Holford et al., 1993).

Advective transport is driven by fluctuations in atmospheric pressure, from synoptic systems and/or winds interacting with the terrain (Kirkham, 2014). More detailed models such as the one used by Holford et al., (1993) utilise this more complex advective-diffusive transport model and appear to effectively model radon diffusion through soil. However, in the case of Holford et al., (1993) the model requires a well measure soil profile and is computationally intensive compared to a steady state diffusive transport model. The lack of input data that would be required, in particular, makes it unfeasible to generalise this type of model to a continental scale.

2.5. Regional radon emissions maps

As research into atmospheric radon modelling has developed there has a been a transition between different methods of characterising radon emissions for different regions. Previously, the most common method used to model radon concentrations was to assume a constant radon exhalation rate of 1 atom cm^{-2} s^{-1} (~21 mBq m^{-2} s^{-1}) for all land masses (Jacob et al., 1997). This method, however, fails to account for the many complexities and dynamics of different land masses such as soil type, soil moisture, local temperatures and radium content, which all play a large role in varying radon emissions on a local scale.

In order to overcome these limitations of using a constant radon exhalation value, it is possible to develop regional emissions/flux maps on a continental scale. These consist of maps displaying radon emissions at the scale of individual sites that attempt to take all these factors into consideration and provide and more detailed and accurate representation of the variation in radon emissions across a continent. The time-dependent nature of these maps also allows for greater analysis of the impact of varying radon emissions on atmospheric radon concentrations. Flux maps have been developed for several regions including Australia (Griffiths et al., 2010), Europe (Karstens et al., 2015) and China (Zhuo et al., 2008), as well as a global radon emission map derived from an amalgamation of regional estimates (Zhang et al., 2011).

2.5.1. Australian radon flux map

The regional flux map that is most relevant to this project is a radon flux map of Australia produced by Griffiths et al., (2010). The aim of developing this map, like all others, was to attempt to improve upon uncertainty in constant radon emissions assumptions for Australia.

Griffiths et al., (2010) created this map (Figure 3) using a diffusive transport model which was calibrated using radon emission point estimates. Inputs for the model including bulk density, porosity, soil texture, radium content, modelled soil moisture (AWAP (Raupach et al., 2009)) and soil temperature.

While the development of this map has provided greater detail for individual sites and a more in-depth understanding of the spatial and temporal variations in radon, it has not yet been shown whether or not the use of a more sophisticated radon emissions map leads to improvements in the simulation of atmospheric radon concentration in transport models.. Further developments are possible with the use of the improved AWRA-L (Frost, 2018) soil moisture model and the inclusion of more data types and data points from updated soil property data, compared with AWAP.

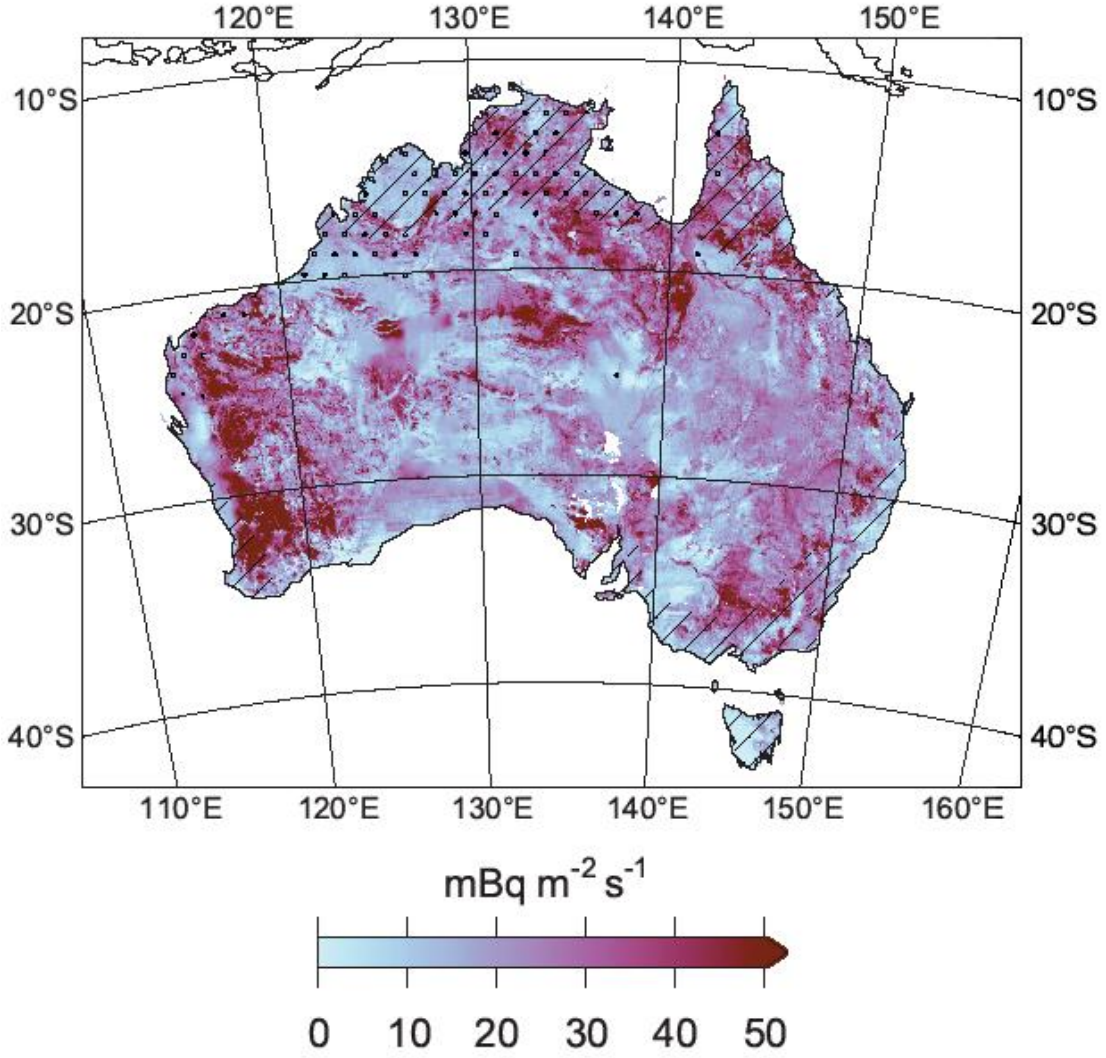

Figure 3: Regional flux map of Australia showing mean radon emissions from 1979 – 2010 (adapted from Griffiths et al., (2010)).

2.5.2. Europe radon flux map

A similar radon flux map has also been developed for Europe in an attempt to improve the accuracy of radon emission estimates across the continent for use in atmospheric transport studies (Karstens et al., 2015). This radon flux map utilises a variety of inputs including soil properties, uranium content and soil moisture.

One of the primary differences with this study is that it produced two emissions maps for Europe based on 2 different soil moisture model estimates (Figure 4). The first is known as GLDAS NOAH and it utilises the NOAH land surface model within the GLDAS (Global Land Data Assimilation System) (Rodell et al., 2004). The second method used comparison is known as ERA-I/L, which utilises the ERA-Interim model as outlined in Balsamo et al., (2015). The large differences between the two land surface models in the Figure 4 clearly show that radon emissions are sensitive to the choice of the soil moisture data product. This soil moisture dependent diffusive transport estimates for this map are based on the Millington and Quirk, (1960) model.

Karstens et al., (2015) found both these soil moisture models to reproduce seasonal trends of radon emissions, with the GLDAS NOAH model showing the closest agreement with observations.

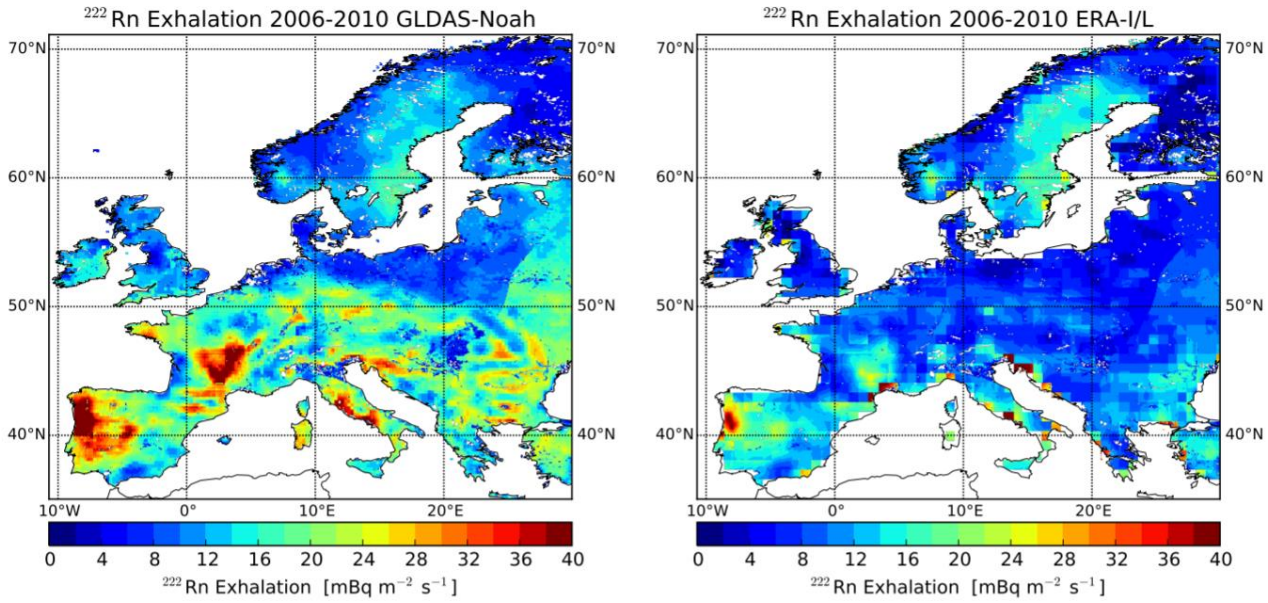

Figure 4: Europe radon flux maps using GLDAS NOAH (left) and ERA-I/L (right) soil moisture models (adapted from Karstens et al., (2015)).

2.5.3. China radon flux map

A radon flux map for China was also developed by Zhuo et al., (2008) to improve upon previously lacking data available for soil radon-222 flux densities across China. The study focused on improving these radon flux estimates by creating a soil radium-226 database and using this alongside the existing global ecosystems database (Zhuo et al., 2008).

This map utilises a previously tested model for radon flux densities which incorporates radium-226 content, soil moisture, soil bulk density, temperature and soil porosity as outlined in Zhuo et al., (2006). Soil moisture in this instance was calculated using a simplified, season dependent soil moisture model which uses an estimation of the dependence of radon emanation power on soil moisture. This differs to the Australia (Griffiths et al., 2010) and Europe (Karstens et al., 2015) flux maps which both utilised spatially dependent soil moisture models as part of their radon flux estimates.

The study found large spatial variations in flux density across China, due to differences in climatic conditions between regions (see figure 5). The overall uncertainty of this model is approximately ±30% with a clear need for improved estimates in future studies.

As with the other maps, more widespread field measurements of radon concentrations will allow for these estimates to be verified more effectively.

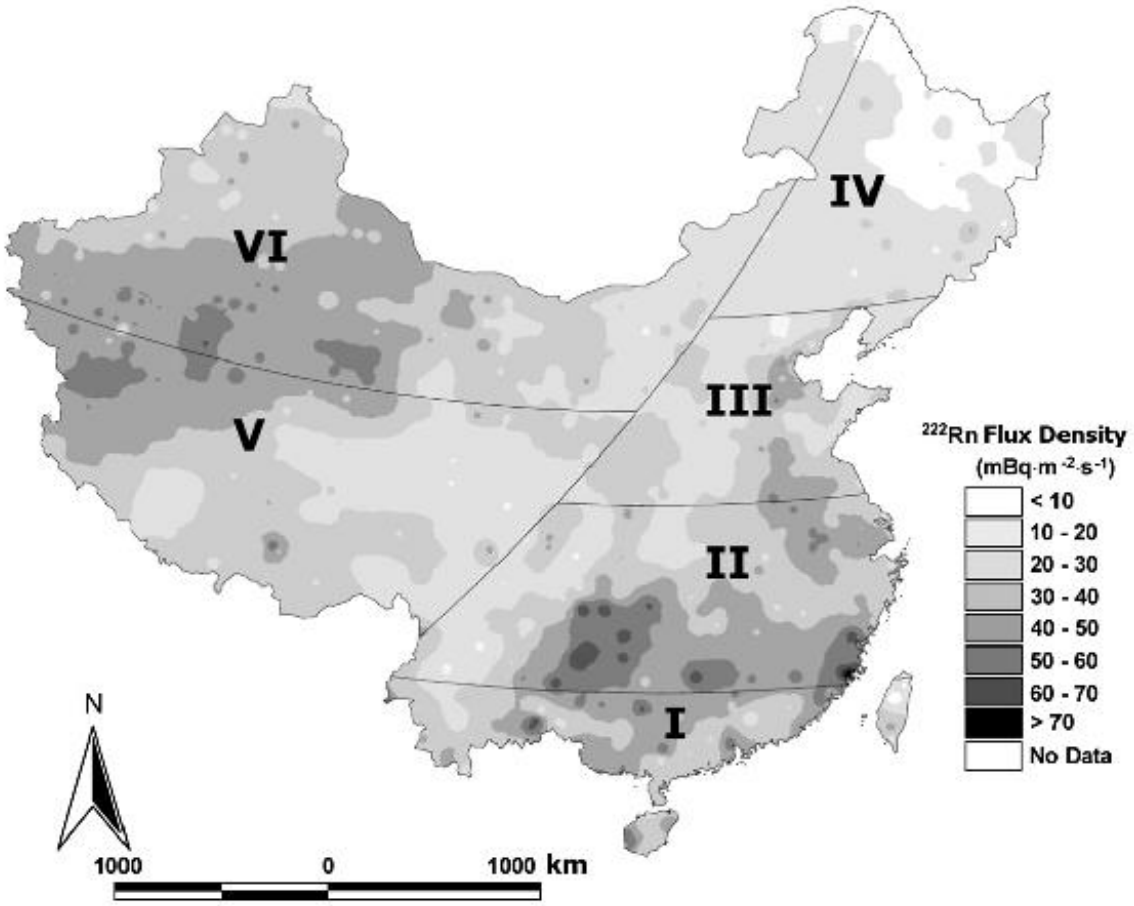

Figure 5: Radon flux map of China showing annual average radon emissions estimates, split into regions based on differences in climatic conditions (adapted from Zhuo et al., (2008)).

In summary, this survey of previous efforts to characterize radon emissions shows:

- There are relatively large spatial variations in radon emissions at continental scale, and at least a factor of 2 difference between regions can be expected.

- Soil moisture plays a key role, and the source of soil moisture data is important.

- Different options exist for parameterising radon diffusivity as a function of soil moisture. Both range from essentially zero when soil is fully saturated, through to maximum diffusivity for dry soil – however they differ in how rapidly they switch between these two extremes.

3. Regional Setting

Much of the motivation behind improving radon modelling comes from its value for understanding the impacts of atmospheric conditions on emissions, specifically those of pollutants, in urban areas, in particular as land uses change and populations expand (Chambers et al., 2015). Having an in-depth knowledge of these processes provides a platform for planning and management regarding pollution within these urban areas.

3.1. Sydney Basin

The Sydney Basin is located in NSW on the east coast of Australia and is comprised of a relatively flat basin bordered by mountains to the north, south and west, and with ocean to the east. The region is named after the city of Sydney, which lies within the basin along the coastline (see figure 6).

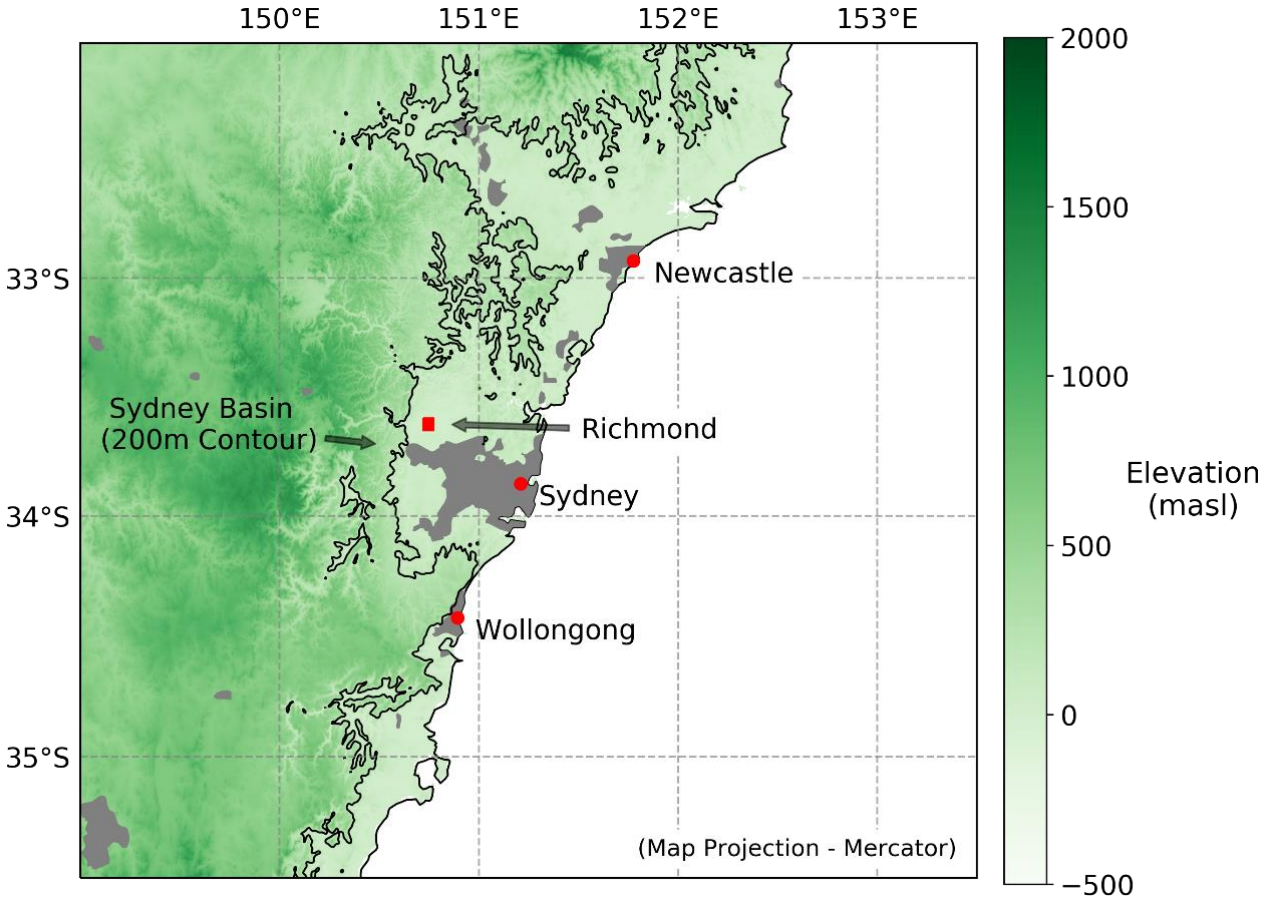

Figure 6: Digital elevation model (DEM) of the Sydney Basin study area, bounded by the 200m elevation contour (thin black line). Urban areas of the region are depicted by grey shading.

The significance of the Sydney Basin as a study area comes primarily from its high population density, with 75% of NSW's population being located in the Greater Metropolitan Area (GMR) (NSW-EPA, 2012). This area encompasses the Sydney Basin, Newcastle and Wollongong regions.

This highly dense population makes it of particular interest due to the large number of people that will be influenced by changes in atmospheric conditions, particularly increases in pollutants and degraded air quality. Thus, attempting to improve atmospheric modelling using localised data allows for a greater understanding of the harmful atmospheric pollutants in the area and their influence on the local population. This modelling is especially important for predicting future changes in air quality.

There are two primary pollutant sources that are most often associated with poor air quality in the Sydney Basin: particulates, especially from bushfires, and ozone from photochemical smog (Horsley et al., 2018).

The first of these pollutant sources involves particles that are smaller than 2.5µm in diameter (PM2.5). These pollutants have been found to be to be a major contributor to human health issues, with the elderly and chronically ill being particularly at risk (Horsley et al., 2018). The potential impact of these pollutants is driven by their source and transport within the atmosphere, thus making it vital to be able to be able to model these events and understand their potential influence. These potentially harmful peaks in pollutant concentrations are primarily driven by the behaviour of the planetary boundary layer (PBL). Locally emitted sources such as traffic and domestic heating generally peak during the early hours of the day when the PBL is still stable and mixing has yet to fully take effect, thus leading to elevated pollutant concentrations.

The second major contributor to reduced air quality within the Sydney basin is ozone which comes as a result of photochemical smog. This smog is a common occurrence in Sydney during summer and levels within the troposphere often exceeds Australian air quality goals (Hart et al., 2006). Hart et al., (2006) showed patterns of the formation of moderate ozone concentrations earlier in the day in western Sydney, with levels pushed even higher later in the day and into the night as sea breezes transport ozone inland from the coastal region. This represents the potential for higher pollution events in the western Sydney area, which is of particular concern as the city expands inland and populations in these areas continue to grow (Greater Sydney Commission, 2018). Understanding

these transport processes and being able to predict flows of pollutants in different scenarios allows for a greater understanding of these pollutants as populations grow and provides a platform for management and planning relating to these changing atmospheric conditions.

3.2. Richmond

The study site chosen for investigating observed radon concentrations is located at University of Western Sydney, Richmond Campus (33.618°S, 150.748°E) (see figure 6). This site is used as a focus area for comparing these radon transport models due to several characteristics. The site is located along the western edge of the Sydney Basin, at the base of the Blue Mountains.

The site is relatively flat, making it representative of a common model grid cell, and is located quite far from the coastline (approximately 55km), with an elevation of 24 m.a.s.l. Due to this, changes in radon concentration at Richmond are more likely to reflect changes in radon emissions than a coastal site, which would be strongly influenced by the local wind direction along with the land-sea contrast in radon emissions.

In addition to the characteristics, the most significant reason for its selection relates to the quantity and quality of data available. Continuous hourly radon measurements have been collected at this site (see Figure 7) using the current detector technology since September 2006 with corresponding climatology and air quality data for much of this time as well (Crawford et al., 2016). These measurements were conducted using the two-filter radon-222 detector as outlined in (Chambers et

al., 2015). The availability of this data has allowed for a detailed assessment of model performance during 2016.

Figure 7: Map of Western Sydney University – Hawkesbury Campus, showing location of radon detectors (Source: Google Earth).

4. Methods

The primary analysis conducted for this study involves a comparison of modelled radon concentrations between four varying radon emissions scenarios. Each of these scenarios have soil moisture estimates of varying degrees of complexity.

A large majority of the time spent for this project involved sourcing an appropriate time-frame for the study period with sufficient data and interesting trends as well as extensively manipulating and analysing data using Python data science tools in order to be able to assess trends and work with the model outputs provided. Much of this process involved developing and implementing new skills relating to Python data science, as this project required the use of several new skills and working with software that I hadn't been exposed to before.

4.1. Soil Moisture Model

The soil moisture data used is derived from the Australian Landscape Water Balance (AWRA-L) daily soil moisture model developed by the Bureau of Meteorology (BOM) (Frost, 2018). This model is a continuously updated simulation of Australian landscape water balance that dates back to 1911. AWRA-L has a 0.05° (approx. 5km) spatial resolution and a daily temporal resolution. It draws from a number of inputs including climate data (wind, air temperature and precipitation), vegetation dynamics and soil properties. The primary output used for this project is soil moisture data for 2016 across 3 distinct soil moisture layers of fixed depths (see Figure 8).

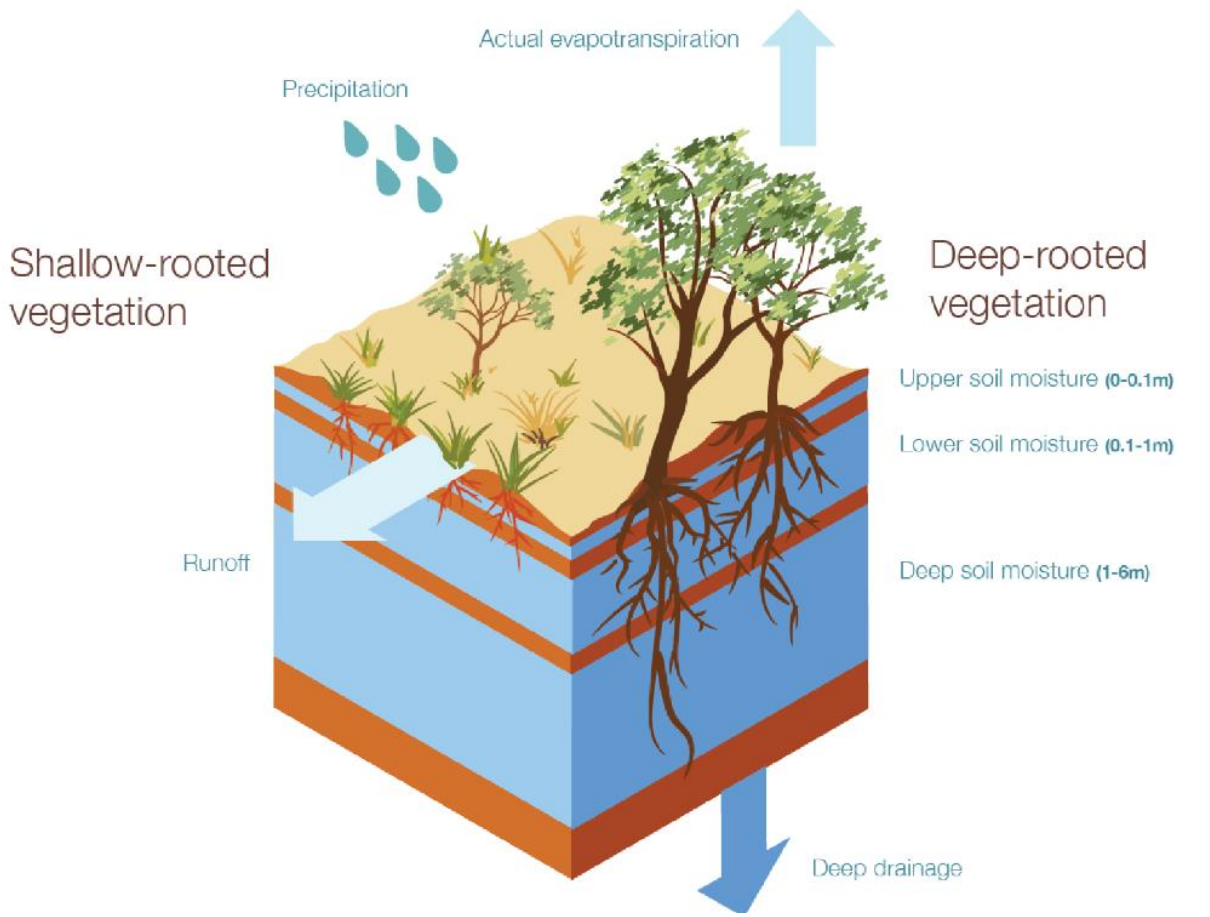

Figure 8: Conceptual diagram of AWRA-L grid cell showing water storage layers and water inflows and outflows (adapted from Frost, (2018)).

This soil moisture model is a more recent development than the previously used Australian Water Availability Project (AWAP) model (Raupach et al., 2009). These models are similar in that they both run across a 0.05° (approx. 5km) spatial resolution, a daily temporal resolution and provide soil moisture data as an output. However, the primary difference is that the AWAP model only reports soil moisture output on a weekly timestep compared to the daily timestep of the AWRA-L model.

Other differences include the vertical discretisation and the data used to derive the spatially resolved input parameters.

4.2. Radon Model

4.2.1. WRF Model configuration

In order simulate transport of radon emissions from the soil and within the atmosphere, a custom version of the Weather Researching and Forecast (WRF) model (Skamarock et al., 2008). This model simulates atmospheric transport from inputs including radon emissions, weather data, soil moisture, temperature etc. The version used for this study is a custom configuration developed by ANSTO and the details of the models are outlined in Figure 9.

Model Identifier	Parameter	W-A11
	Research Group	ANSTO
Model specifications	Met. model	WRF
	Chem. model	WRF-Chem with simplified Radon only
	Met model version	3.7.1
Domain	Nx	80, 73, 97, 103
	Ny	70, 91, 97, 103
	Vertical layers	50
	Thickness of first layer (m)	19
Initial & Boundary conditions	Met input/BCs	ERA Interim
	Topography/Land use	Geoscience Australia DEM for inner domain, USGS elsewhere. MODIS land use
	SST	High-res SST analysis (RTG_SST)
	Integration	Continuous with 10-d spin up
	Data assimilation	Spectral nudging in domain 1 above the PBL (scale-selective relaxation to analysis)

Model Identifier	Parameter	W-A11
	Research Group	ANSTO
Parameterisations	Microphysics	WSM6
	LW radiation	RRTMG
	SW radiation	RRTMG
	Land surface	NOAH
	PBL	MYJ
	UCM	Single layer UCM
	Convection	G3
	Aerosol feedbacks	No
	Cloud feedbacks	No

Figure 9: Details of WRF-CHEM meteorological model used for this study (adapted from (Monk et al., 2019)).

The model is the same configuration used by Griffiths et al., (2010). In this instance, the model was run 4 times encompassing the varying emissions scenarios. Each of the soil moisture driven model runs utilised the radon emissions model developed by (Griffiths et al., 2010).

The motivation for developing this model was for its use as part of the Sydney Particle Study and a comparison of radon WRF-CHEM models (Monk et al., 2019).

For the purpose of this study, all emissions and concentration maps were run across domain 3 which has a 9km spatial resolution.

4.2.2. Emissions scenarios

The WRF-CHEM model was run Australia wide using four different emissions scenarios that each vary in their estimation of radon emissions. This variation is primarily based on the degree to which soil moisture is taken into consideration and the complexity of the soil moisture data. By varying these parameters, it is possible to compare each of these scenarios and how they perform in different conditions.

Table 1: Summary of key properties for each emissions scenario used.

Emissions Scenario	**Constant**	**Average**	**Weekly**	**Daily**
Temporal Resolution	N/A	N/A	Weekly	Daily
Spatial Resolution	N/A	0.05° / ~5km	0.05° / ~5km	0.05° / ~5km
Soil Moisture Model	N/A	AWAP	AWAP	AWRA-L

The four model emissions scenarios were assigned names based on their characteristics: ‘Constant’, ‘Average’, ‘Weekly’, and ‘Daily (in order of increasing complexity). These can be divided into two categories based on their temporal characteristics, with the ‘Constant’ and ‘Average’ scenarios being non-time dependent, while the ‘Weekly’ and ‘Daily’ scenarios are time dependent.

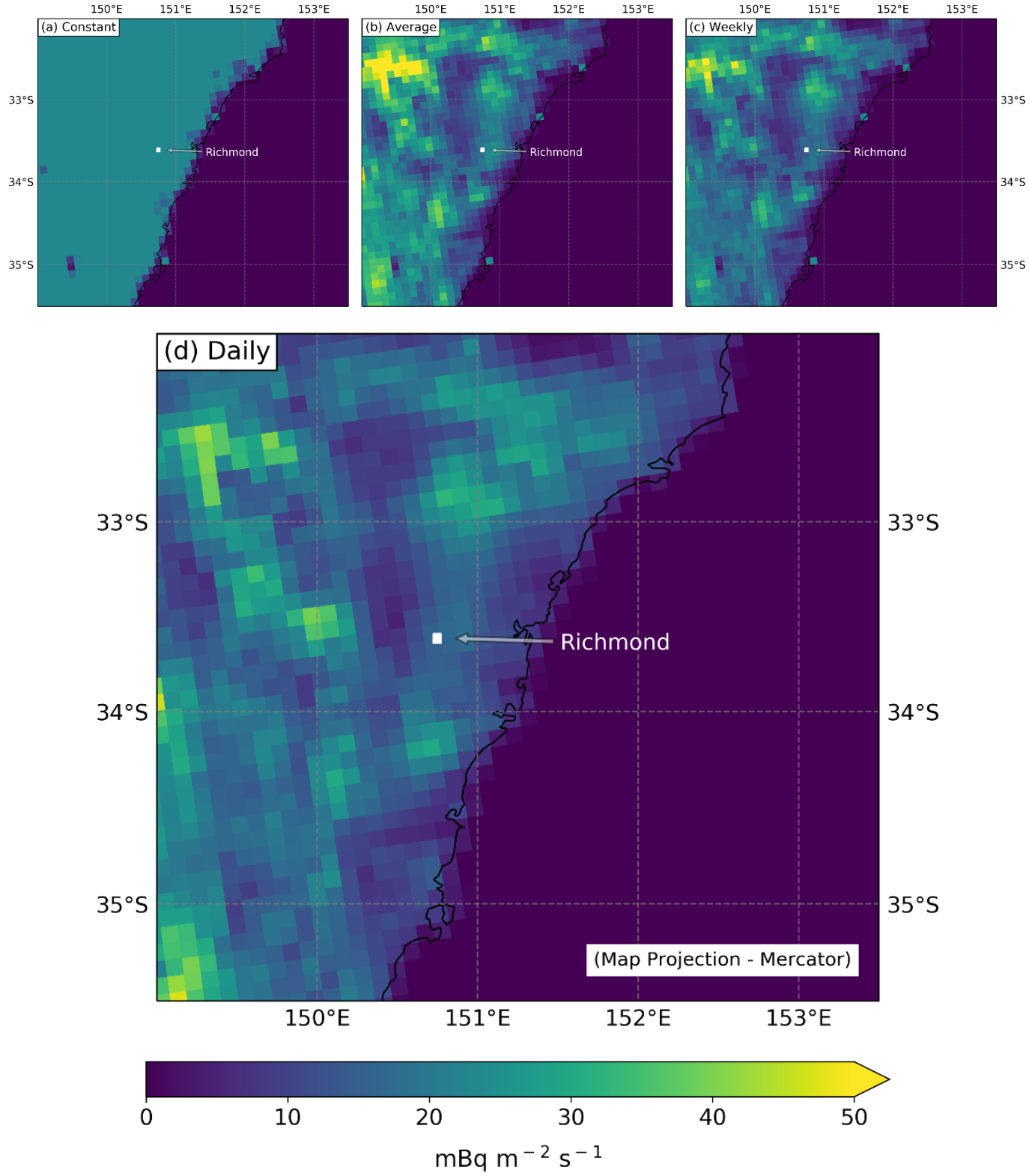

Figure 10: Maps of radon emissions of Australia from domain 3 for four emissions scenarios: a) Constant emissions, b) Average emissions), c) Weekly emissions, d) Daily emissions.

The ‘Constant’ emissions scenario, shown in Figure 10a is the most simplistic representation of radon emissions of the four scenarios. These radon emissions are spatially and temporally constant and are based on a single value for radon emissions. The value of radon emissions used for this scenario is 23.4 mBq $m^{-2}s^{-1}$ for all of Australia, based on mean radon emissions from the radon emissions map of Australia created by Griffiths et al., (2010). This value is an average of the map over space and time for the period of 1979 to 2010. This represents the previously widespread method of assuming constant radon emissions for an entire landmass (Jacob & Prather, 1990).

The ‘Average’ emissions scenario, shown in Figure 10b is the next most complex of the four scenarios. The emissions for this scenario are spatially variable based on the Australian radon emissions map from Griffiths et al., (2010) with a spatial resolution of 0.05° or ~5km, but the emissions are constant with time based on a 30-year average of this map. The soil moisture data for this map is derived from the AWAP soil moisture model (Raupach et al., 2009). The value of radon emissions derived from the Richmond study site using this scenario is ~17.4mBq $m^{-2}s^{-1}$.

The ‘Weekly’ emissions scenario, shown in Figure 10c is the first of the time-dependent emissions scenarios used. This scenario varies both spatially and temporally and utilises the emissions map of Australia from (Griffiths et al., 2010). It has a weekly temporal resolution, defined by the AWAP soil moisture model that is being used (Raupach et al., 2009). These emissions are also spatially variable across Australia with a spatial resolution of 0.05° or ~5km. Soil moisture data for this model is split into two distinct soil layers and the depth of each layer varies based on the depth of the topsoil and subsoil as defined by the Atlas of Australian Soils.

The ‘Daily’ emissions scenario, shown in Figure 10d is the final and most complex estimation of radon emissions used. The emissions for this scenario are derived from a new radon flux map which was developed by ANSTO for this project (A Griffiths, 2019, pers. comm.) with its primary improvement being its use of newer AWRA-L soil moisture model which has 3 layers of modelled soil moisture and fixed soil layer depths (Frost, 2018). Compared to the ‘weekly’ emissions scenario, this scenario utilises the Millington and Quirk, (1960) parameterization recommended by Karstens et al., (2015). Both the map itself and the AWRA-L soil moisture model also benefit from additional data sources and updated input data.

Each of these emissions scenarios will be used to determine how atmospheric radon concentrations respond to changing conditions, based on the complexity of soil moisture data.

4.3. Observations

4.3.1. Radon

The radon-222 observation data for this study has been obtained from continuous radon measurement campaigns conducted at the Richmond study site (see Figure 11), as described in Section 3.2. The measurements for this study were taken as part of long term radon monitoring efforts with the introduction of the currently used two-filter radon detector in 2006 (Crawford et al., 2016). During this time there have been intensive measurement campaigns, such as the Sydney Particle Study, which have involved the collection of large amounts of radon and other atmospheric pollutant data for target time periods (Cope et al., 2014). Results for this study are taken from the 1-year period of 2016 exclusively.

Figure 11: Close up map showing location of Richmond measurement site (Source: Google Earth).

4.3.2. Radon Detector

The instrument used for detection of atmospheric radon concentrations used in this study is based on the dual flow loop, two-filter detector, commonly referred to as the two-filter detector (see Figure 12. This design was developed by Whittlestone and Zahorowski, (1998) and has become widely deployed for low-level ambient radon measurements, in particular as part of the World Meteorological Organisation Global Atmospheric Watch program (Chambers et al., 2016; Zahorowski et al., 2004)

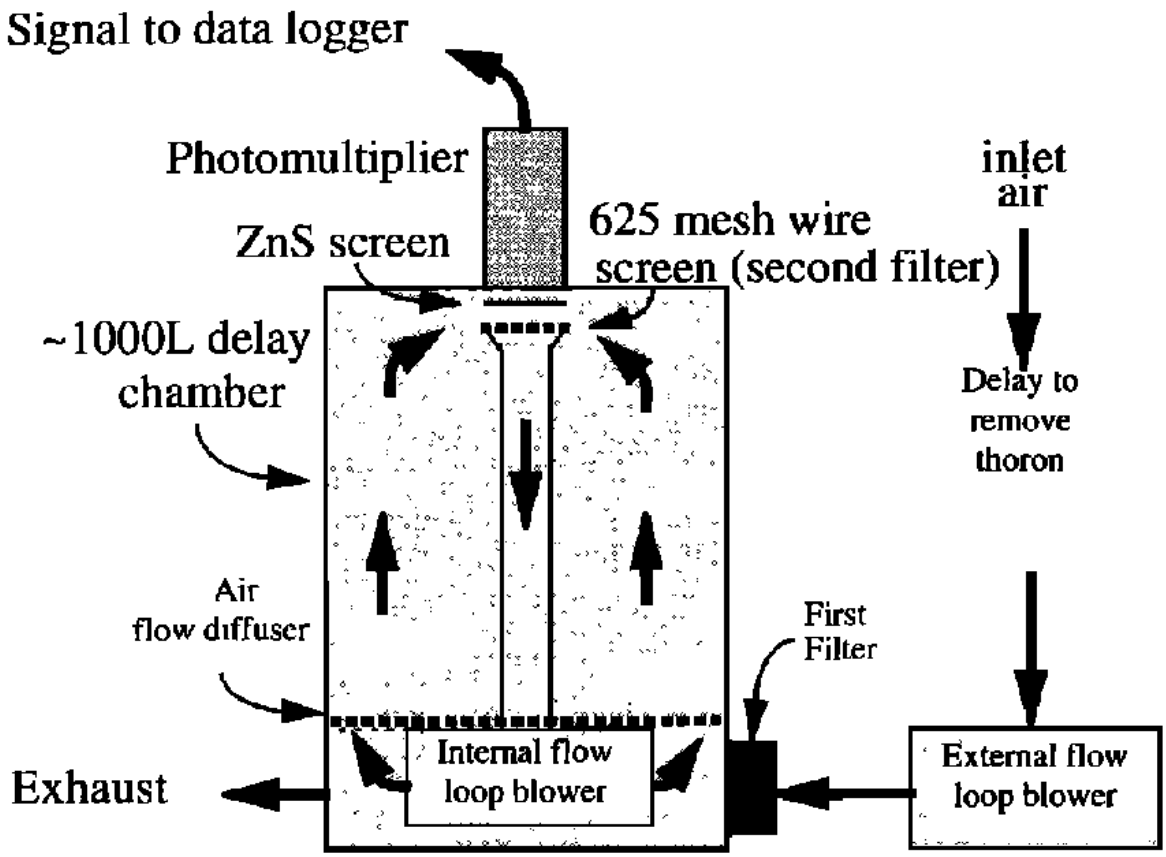

Figure 12: Schematic of original dual-flow loop two-filter radon detector design (adapted from Whittlestone and Zahorowski, (1998)).

This detector has an advantage over other methods, as it takes direct measurements of radon concentration, rather than indirect detectors which instead derive the radon concentration from the ambient concentration of radon progeny. While indirect measurements do have benefits for low-concentration radon measurements, in this instance direct measurements are favourable because

the concentration derived isn't dependent on external corrections or assumptions, as is the case for single filter detectors (Griffiths et al., 2016).

As outlined in Chambers et al., (2015), measurements at Richmond were made using a 1500L dual-flow loop, two-filter detector (see Figure 13), with continuous direct measurements being made on an hourly basis. Calibrations of the radon detector were conducted every 3 months using a constant radon source, with an approximate variability of 5% for calibration coefficients (Chambers et al., 2015).

Figure 13: Dual-flow loop, two filter detector used at the Richmond study site for collection of radon concentrations (Credit: ANSTO).

A consideration that must be made when using dual-flow loop, two-filter detectors is their slow response time. Griffiths et al., (2016) developed a correction for this delay which uses a Bayesian deconvolution method to adjust measurements to their correct time. However, in this instance, the correction was not applied to the radon observation data as the degree to which this correction affects the data is not significant when comparing to the large error of modelled radon concentrations.

4.3.3. Climatological Data (NSW OEH)

Alongside the continuous hourly radon concentration measurements being made at the Richmond study site, climatological data was also collected to allow for comparison with the radon measurements. The data types that were collected include temperature, wind speed and wind direction. These measurements were conducted at a site adjacent to the location of the radon measurements and provided by the NSW OEH.

Temperature data was collected at an hourly interval at approximately 5m above ground level, while wind speed and direction data were collected at an hourly interval at approximately 10m above ground level (see Figure 14).

This data is used to assess the impact of each of these climatological parameters on the performance of modelled radon across each of the emissions scenarios, as well as comparisons with the data used during the model simulation.

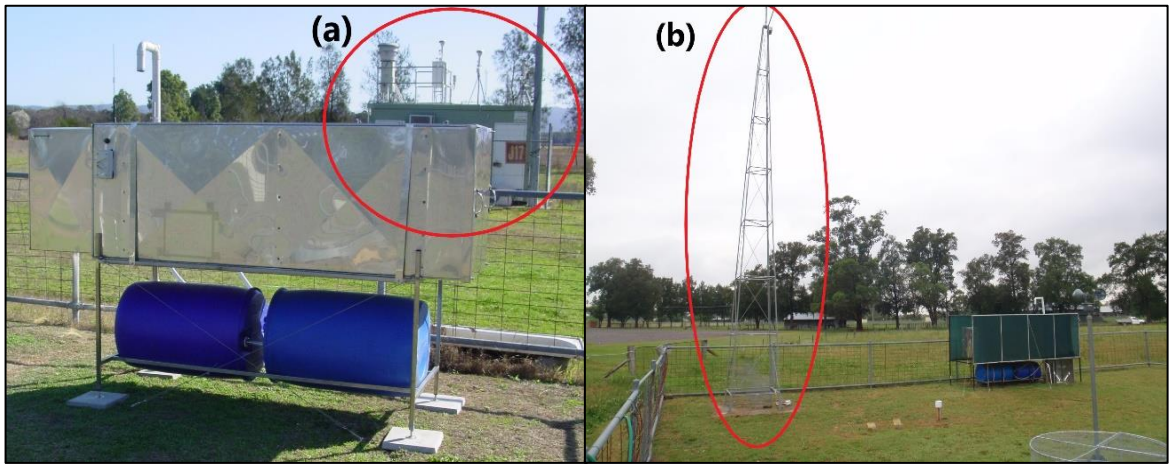

Figure 14: Instruments used to measure climatological data at Richmond study site: a) temperature, b) windspeed and direction (Credit: ANSTO).

Daily rainfall data was gathered from the Bureau of Meteorology in order to establish timeframes of major rainfall events during the year.

5. Results & Discussion

5.1. Rainfall

Developing an understanding of the rainfall trends during the study period is essential in order to undertake an effective analysis of modelled radon concentrations. The rainfall data being used is from the Bureau of Meteorology (BOM) an taken from the nearby Richmond RAAF Base rather than the Richmond UWS study site being used for the rest of the analysis (BOM, 2019a;2019b). This is primarily due to lack of complete, daily updated rainfall data at the UWS study site, compared the much more comprehensive data available at the Richmond RAAF Base. The data collected at this site will be very similar due to the sites being only approximately 4km apart.

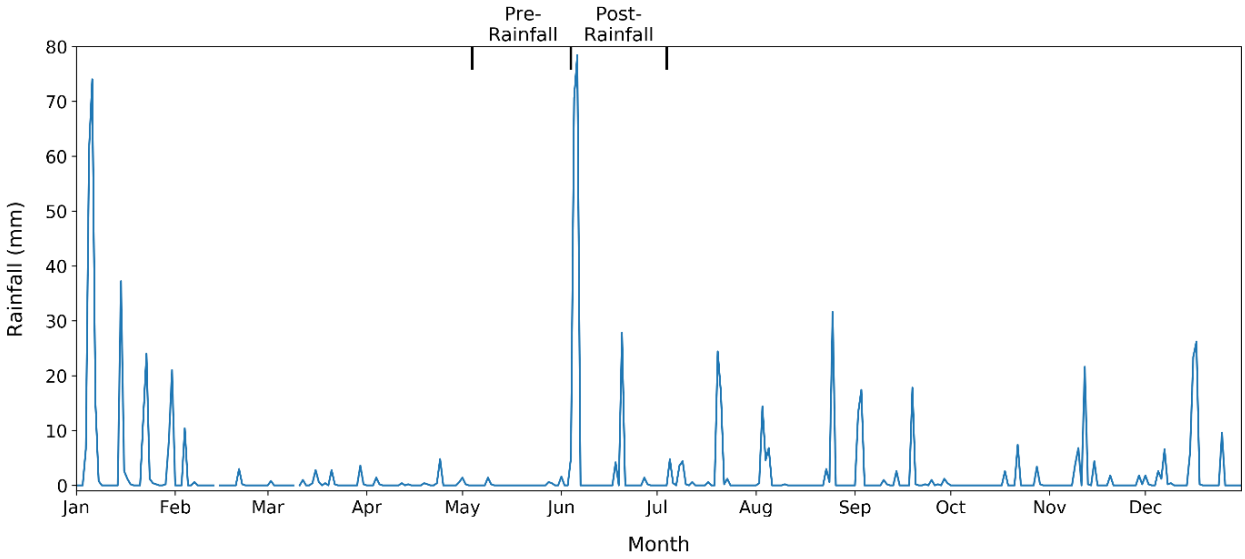

Figure 15: Daily rainfall data for 2016 taken at Richmond RAAF Base (Source: BOM, (2019a))

I undertook an initial search over several years of observations to find a period which had both high-quality radon observations, and a wide range of soil moisture. Other periods were initially considered, however could not be used due to insufficient observations available.

These criteria were fulfilled in 2016, as shown in Figure 15 which depicts the patterns of rainfall at Richmond throughout 2016. There are two clear rainfall events that occurred during the year which are likely to have the greatest impact on soil moisture in the area. The first is during January and exhibits a large rainfall event of 158mm over 5 days at the beginning of the month. This is followed by several subsequent smaller rainfall events with decreasing magnitude through the rest of the

month. The second major rainfall event observed during 2016 occurred at the beginning of June from the 4th to the 6th of the month, with a total 154mm over 3 days.

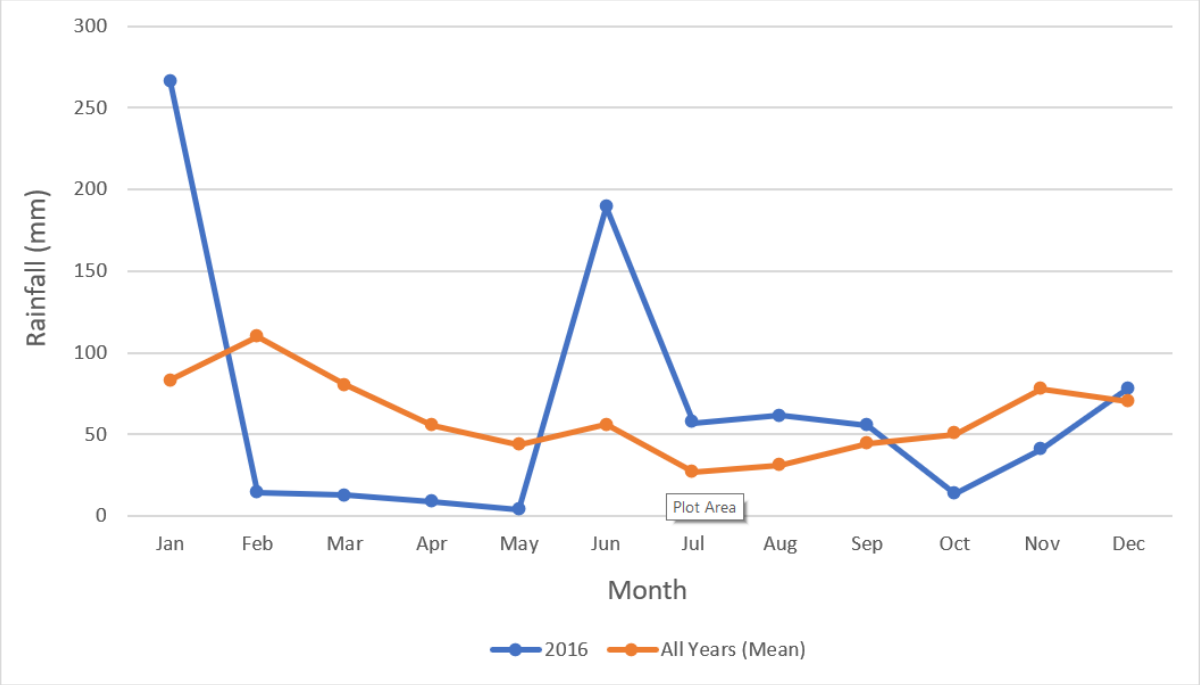

Figure 16: Monthly comparison of rainfall data for 2016 compared to the long term average (Source: BOM, (2019b)).

While this event is quite similar to the first, it is of particular interest as it occurs following a several month period of low rainfall with a total of only 39.8mm over the 4 months prior from February to May. When compared to the long-term averages of monthly rainfall as displayed in Figure 16 it is clear that this is a period of abnormally low rainfall as it sits well below the long-term averages for those months. Similarly, the total rainfall for June 2016 of 189.2mm is abnormally high when compared to the long-term average of 55.9mm, which is primarily driven by the rainfall event seen in Figure 15 at the beginning of June.

This sharp transition from extremely dry conditions to extremely wet conditions is ideal for examining the response of modelled radon concentrations to soil moisture as it provides a clear transition from dry soil conditions to wet soil conditions. By comparing radon concentrations before and after this rainfall event will provide an insight into how each of the emissions scenarios handles soil moisture.

Thus, this rainfall event will be used as a focus time period for the remainder of this study and will be referred to as the 'major rainfall event' and will be indicated by a red-dotted line on all future plots. In order to analyse the differences before and after this event, two-month long time periods, on

each side of the event, have been chosen for more in-depth analysis. The first will be referred to as the 'Pre-rainfall' and extends from the 4th of May to the 4th of June, while the second time period will be referred to as 'Post-rainfall and extends for the 5th June to the 4th July. These time periods will also be marked on all future plots.

5.2. Modelled Soil Moisture

As soil moisture dynamics and their influence on modelled radon concentrations are the primary focus of this study, it is necessary to examine their trends, in order to act as a basis for the response of radon to changes in soil moisture. As previously stated, soil moisture data is taken from a subset of the AWRA-L model output taken from the grid-cell that encompasses the Richmond study site. All data has also been scaled according to the depth of the layer in which the soil moisture is present to allow for comparison. This represents one of the more recent soil moisture models currently available from Australia and is the soil moisture input used in the Daily radon emissions scenario.

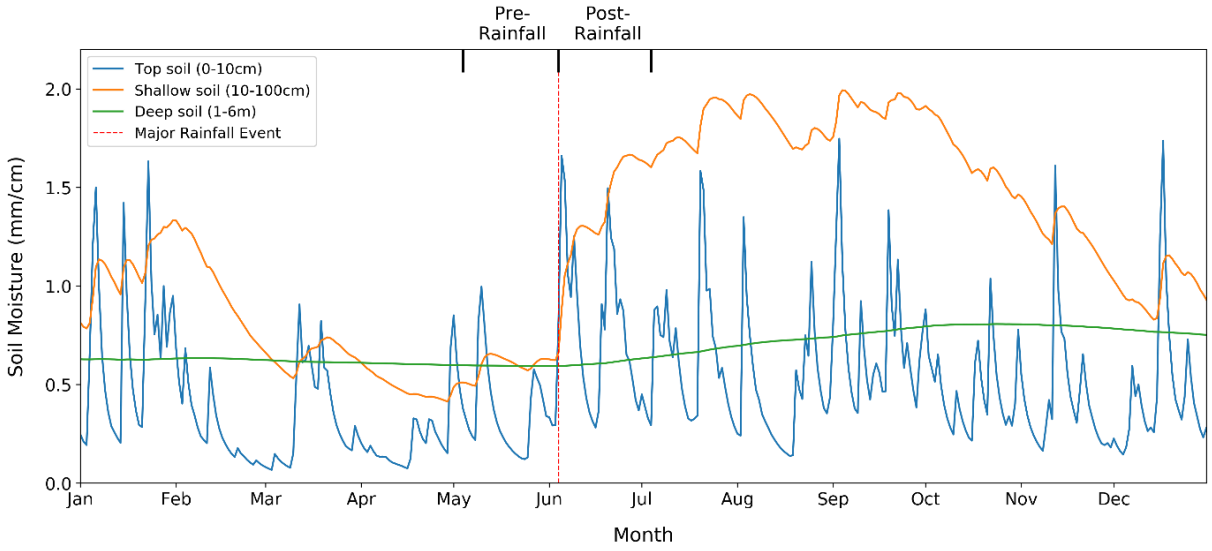

Figure 17: Soil moisture data for 2016 taken at the Richmond study site. Data is derived across 3 layers (top soil, shallow soil and deep soil) from the AWRA-L soil moisture model (Frost, (2018)).

Figure 17 shows the response of each of the 3 soil moisture layers present in the model to the aforementioned rainfall events. As alluded to previously, the most significant change in soil moisture occurs following the June major rainfall event, in which there is an increase across all three layers, albeit all to different extents. Figure (Soil Moisture Timeseries) also provides an insight into the characteristics of each of the layers and their vastly varying response to major rainfall events.

The top-soil moisture (0-10cm) is the layer closest to the surface and as seen throughout 2016 this layers exhibits a large and rapid response to rainfall events; however, this is short lived as the moisture evaporates or drains to lower layers. In this instance, the response of this layer to the June major rainfall event is an increase from 0.3mm/cm to 1.66mm/cm at its peak, however this is followed by a decrease back to 0.3mm/cm approximately a week after the event.

The shallow-soil moisture (10-100cm) is the second layer from the surface and responds significantly different to the layer above. This layer generally responds slower than the above layer and is generally more stable than the above layer. Figure 17 shows this with an increase from ~ 0.6mm/cm prior to the major rainfall event to ~1.3mm/cm post-rainfall. These increased levels remain stable until subsequent rainfall events which cause smaller more incremental increases, until it reaches a maximum which fluctuates around ~1.9mm/cm through to September, at which point soil moisture is this layer starts to decrease. The variability in this layer, which is quite large, persists over a period of several months

The deep-soil moisture (1-6m) is the third and lowermost layer of the AWRA-L soil moisture model. This layer shows a significantly slower response to the major rainfall event and shows a gradual increase over several months from 0.6mm/cm to 0.8mm/cm and aligns generally with the changes in the above layer.

While considering these soil moisture dynamics at the Richmond study site, it is also important to consider how these compare spatially to the rest of the region, as the spatial variability of Richmond are likely to play a role in soil moisture levels.

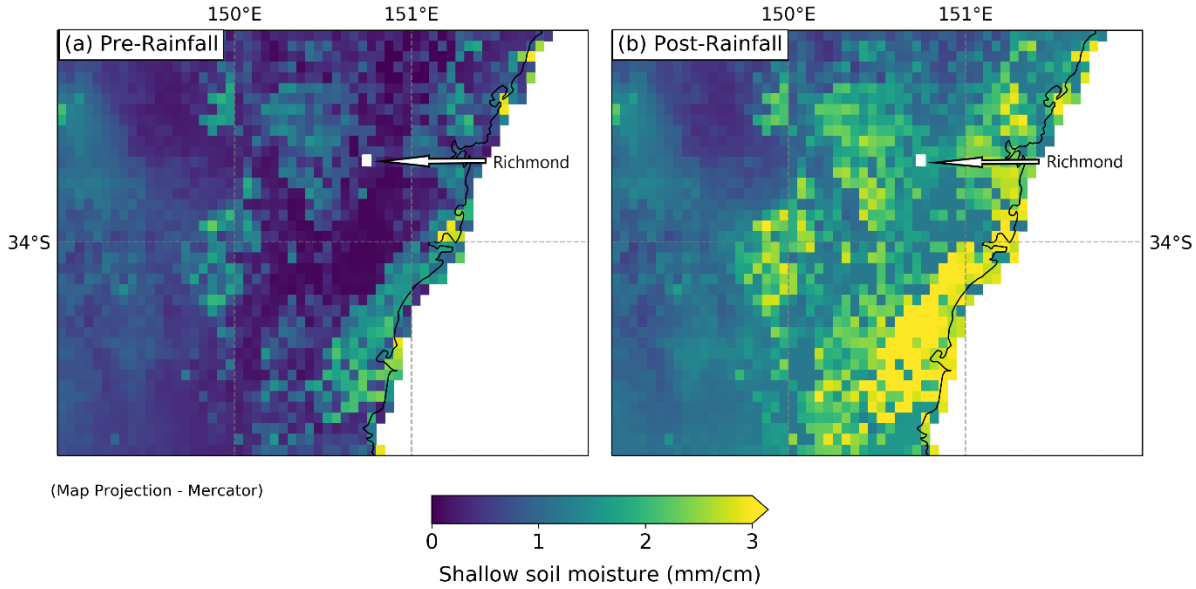

Figure 18: Surface soil moisture map for the Sydney Basin depicting soil moisture a) before (4th June 2016) and b) after (6th June 2016) a major rainfall event.

There are clear spatial differences between the Richmond study site and the rest of the region both pre-rainfall and post-rainfall (see Figure 18). The Richmond study site is in an area of lower soil moisture compared to the higher values for escarpment to the west and the coast to the east. These patterns remain consistent after the major rainfall event and soil moisture levels appear to increase uniformly across the region in response.

5.3. Observed Radon

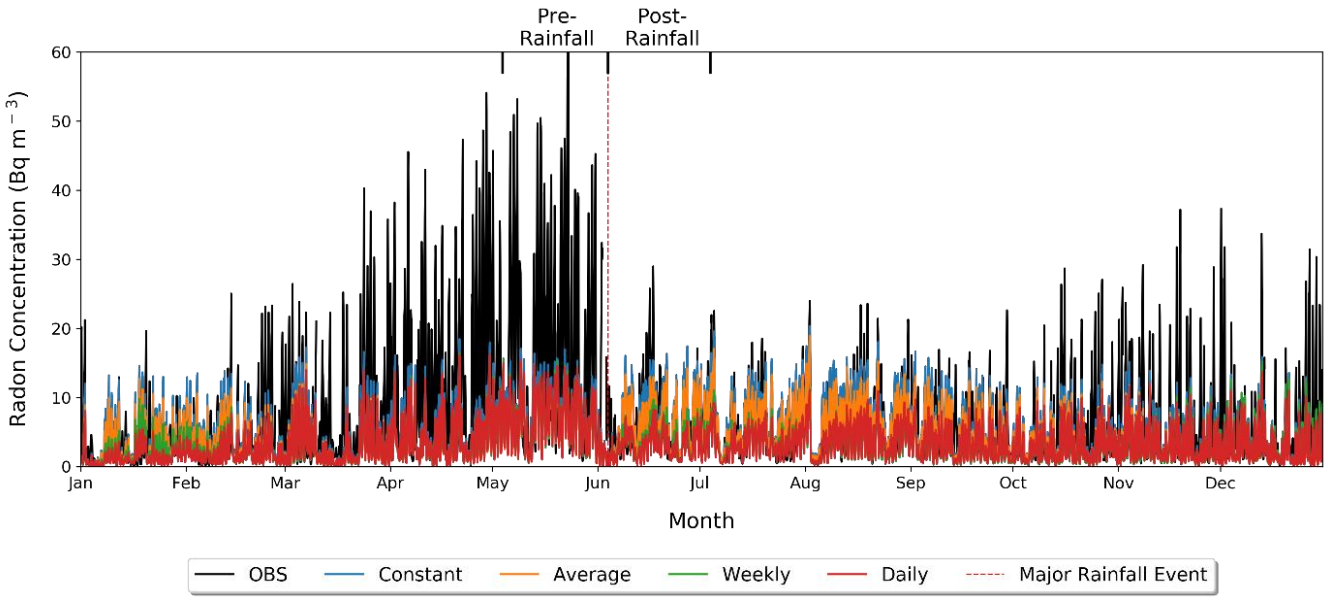

Figure 19: 2016 radon concentrations taken from the Richmond study site from observation and the 4 emissions scenarios.

Radon concentrations measured at Richmond between January and December 2016 show significant fluctuations throughout the year with a minimum of 0.09 Bq m^{-3} and a maximum of 73.55 Bq m^{-3}.

As time from the last major rainfall event increases, the maximum radon concentrations also increase. This is shown in Figure 19 from March to June 2016 as radon concentrations recover from a rainfall event in January. A second occurrence of this is visible mid-way through October as soil moisture decreases again following the June major rainfall event.

Table 2: Summary of observed radon concentration data for 2016

Time Period	Minimum concentration (Bq m^{-3})	Maximum concentration (Bq m^{-3})	Average concentration (Bq m^{-3})
All time	0.09	73.55	6.89
Day (12pm – 3pm)	0.09	15.74	2.22
Night (4pm – 11am)	0.09	73.55	7.81

The average for this period was 6.89 Bq m^{-3}. Much of this is driven by night-time (4pm-11am) radon concentrations as Table 2 shows much lower values for the day-time period with an average of only

2.22 Bq m^{-3}. This is primarily driven by the shallower nocturnal boundary layer present during cooler night-time conditions, which reduce the ability of radon to be mixed vertically (Chambers et al., 2011). Alternatively, daytime conditions (12pm-3pm) exhibit the much deeper convective boundary layer which allows for large amounts of mixing and transport and thus reducing surface radon concentrations. This is the time at which the atmosphere is the least stable and isn't being influenced by the nocturnal boundary layer.

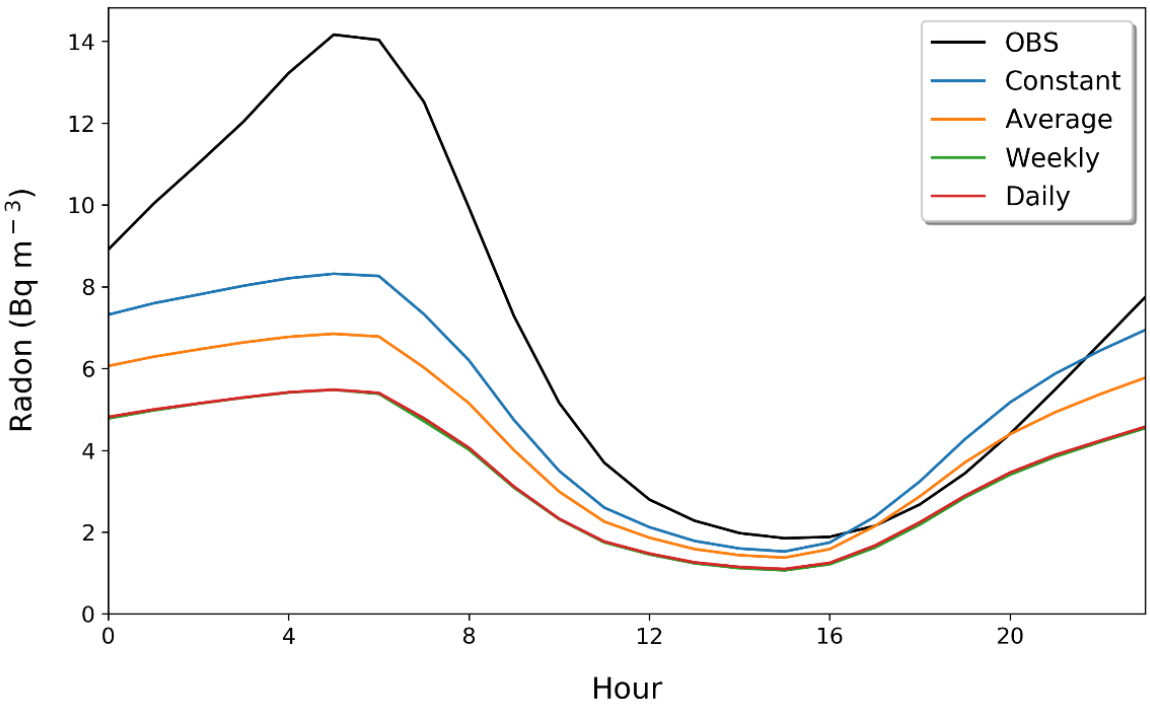

Figure 20: Mean 2016 diurnal cycle of radon concentrations for observations and 4 emissions scenarios.

The average diurnal variations in radon concentrations throughout the year, as shown in Figure 20, exhibit a trend of fluctuating radon concentration with time of day and the large variations that are caused by the shift in the planetary boundary layer height. This pattern and the night-time peaks are one of the most influential factors in limiting the accuracy of modelled radon, as the model currently in use does a poor job at simulating these conditions.

5.3.1. Response of radon concentrations to soil moisture variations

Figure 19 shows distinct extended periods of both heightened and lowered radon concentrations which are apparent throughout the year, apparently in response to changing soil moisture conditions. April to June shows a period of heightened radon concentrations as soil is deprived of moisture and the barrier to diffusion is lowered. This is followed by a significant drop following the major rainfall event in June, which is sustained until October as the moisture in the soil remains as a result of subsequent smaller rainfall event.

This response of radon to soil moisture is by increased saturation of the soil, leading to reduced pore space and limiting the available space for radon to transport through the soil. Previous studies (Ishimori et al., 2013; Rogers & Nielson, 1991) have shown this relationship between soil moisture saturation and diffusion of radon through soil, with the pattern showing an exponential decline in the radon diffusion co-efficient as the fraction of saturated soil increases. This results in a physical blocking of radon from undergoing diffusion through soil.

5.4. Modelled Radon

5.4.1. Performance of emissions scenarios

Modelled radon concentrations for each of the four emissions scenarios run produced varying results. While all model runs differ significantly from the observed values, when compared against each other, the performance differences for each of the scenarios can be seen. Spatially the models also differ in their representation of radon concentration (see Figure 21). The constant scenario produced less distinct spatial differences across the Sydney basin, with less distinction between areas of higher and lower mean radon concentration. This is due to the spatially constant nature of this scenario. One important result from Figure 21a is the large amount of spatially variability present particularly in Western Sydney, even for the constant emissions scenario, primarily driven by the atmospheric transport of radon by the model.

Alternatively, the ‘average’ emissions scenario (see Figure 21b) shows more distinct spatially variations in radon concentrations, due to the availability of spatially variable emissions. However, there are still some features common to both scenario types, with large valleys alongside the western edge of the basin which are likely to be region of nocturnal drainage flows. The shows the large degree to which spatial variability of radon concentration is due to meteorological factors.

Lower concentrations are shown across the domain for both the time dependent scenarios, as these have both considered the major soil moisture influence throughout the year.

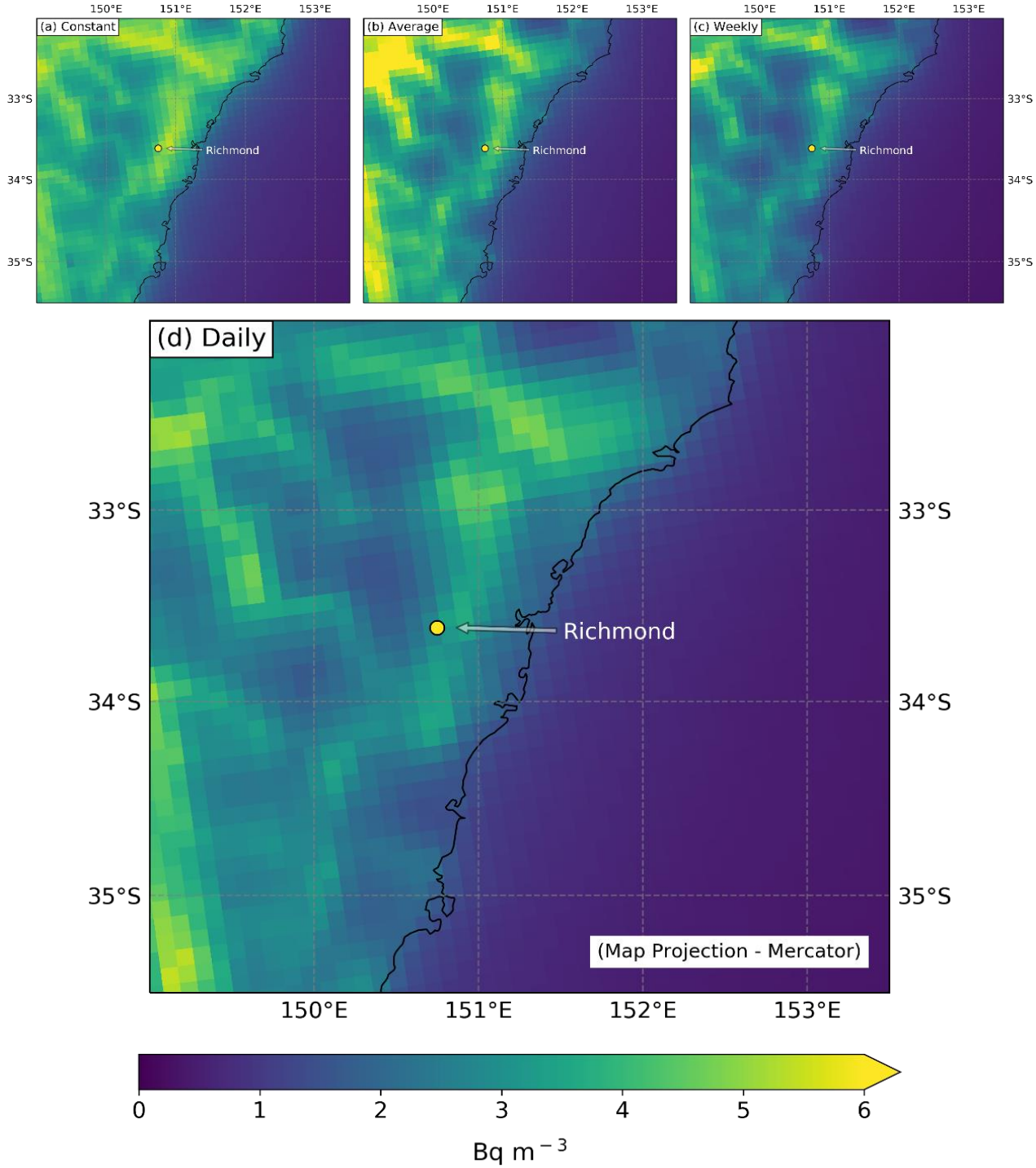

Figure 21: Maps of radon concentrations of Australia from domain 3 for four emissions scenarios: a) Constant emissions, b) Average emissions), c) Weekly emissions, d) Daily emissions. Yellow dot represents average radon concentration for 2016.

Figure 22 shows a correlation scatter plot for each of the four emissions scenarios against observed values. The first pattern that is apparent is a divide between the two non-time dependent and the two time-dependent scenarios. The constant and average scenarios performed worse than the other

two, each with a correlation co-efficient of 0.55 and 0.54 respectively. The two time-dependent scenarios, weekly and daily, both showed a higher correlation score of 0.67 and 0.68 respectively. Despite these differences, the clear variation can be seen in the spread of the scatter plots in Figure 22. When comparing the two types, the time-dependent scenarios appear to both have a tighter spread of values and are simply offset by a small amount and generally underestimate modelled radon concentrations. There are several possible explanations for this trend, the first being the ability of these scenarios to respond to changes in soil moisture, which isn't present in the non-time dependent scenarios, and allows for a higher correlation of values. A second explanation of this pattern relates to the sparsity of radium-226 data available for the Sydney basin, forcing these values to be interpolated from surrounding regions and potentially not entirely representative of the Richmond area in particular. One final possible cause is due to the heavy bias present in the nocturnal mixing height, which is poorly estimated by all emissions scenarios and leads to an average underestimation of radon concentrations during night-time (see Figure 23).

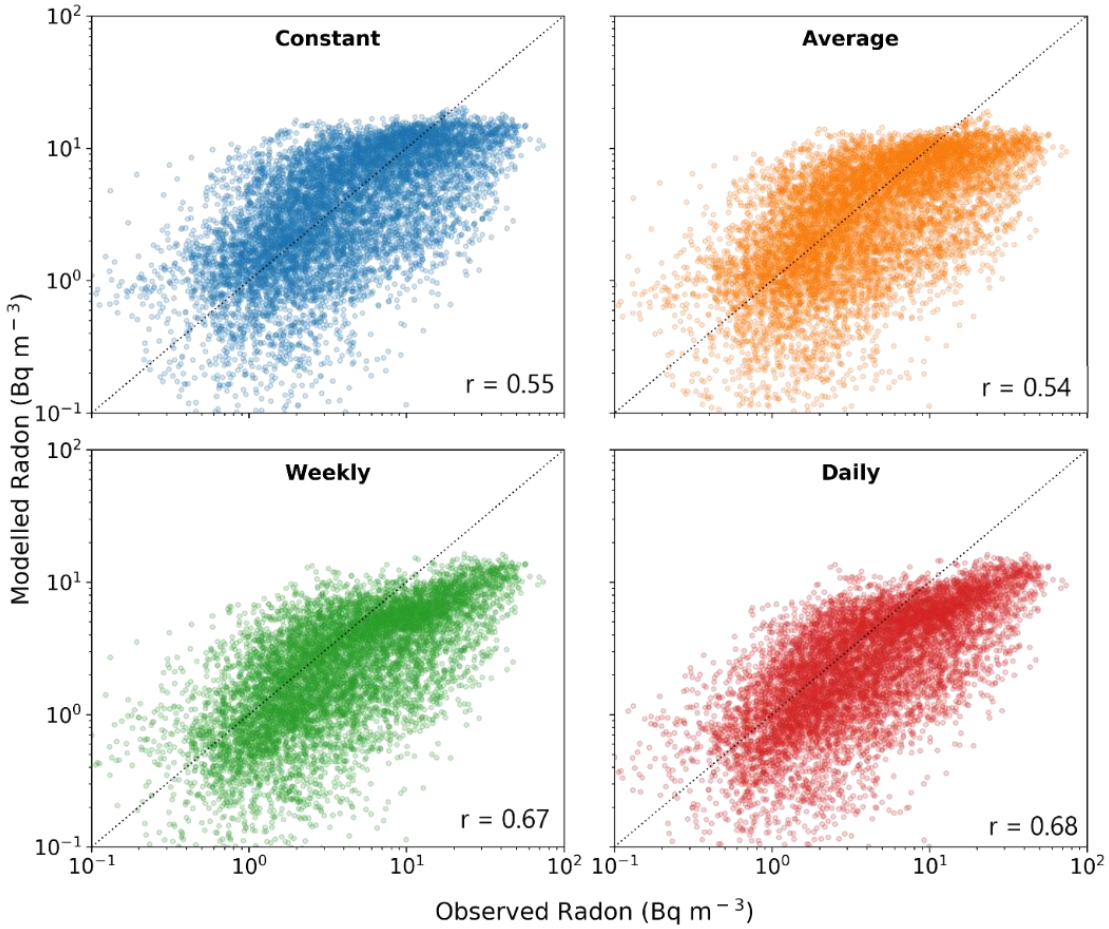

Figure 22: Scatter plots showing correlation of modelled radon and observed radon for 4 emissions scenarios for 2016.

Alternatively, the two non-time dependent scenarios show a wider spread of values and less of a consistent trend relative to the ideal fit (r=1). This is the case because while the non-time dependent scenarios cannot respond to the rainfall events, at certain times their estimates line up with observed values as can be seen in Figure 19 during July after the major rainfall event. This is primarily due to the average emissions estimates found at Richmond encompassing a large proportion of wet time-periods, leading to these non-time dependent scenarios producing radon concentrations similar to those seen post rainfall. However, despite Figure 19 showing a similar magnitude to the observed radon concentrations post rainfall, the correlation of individual measurements is still largely inconsistent (see Figure 22).

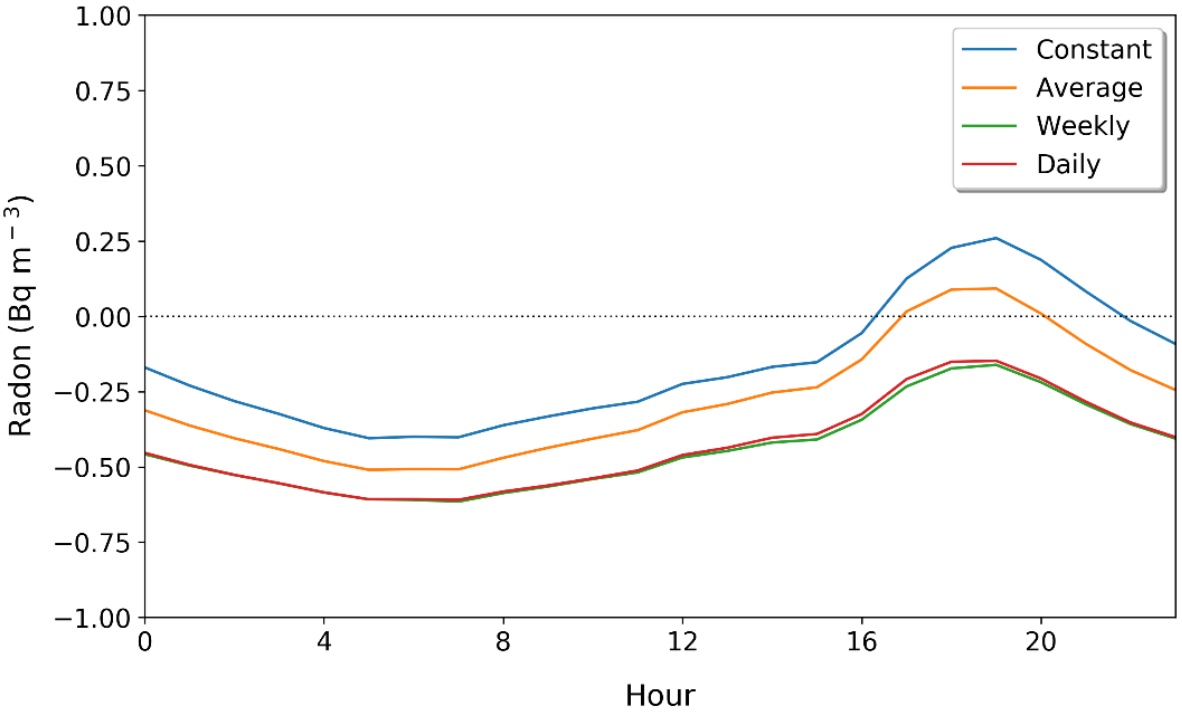

Figure 23: Diurnal Normalised Mean Bias (NMB) for 2016 for 4 emissions scenarios.

Another measure for assessing the performance of each of the emissions scenarios was undertaken by comparing normalised mean bias in relation to observed concentrations. Figure 23 shows that the time-dependent models both performed very similarly, ranging from a normalised mean bias of -0.5 to -0.25. Alternatively, while both non-time dependent scenarios trend closer to the observed values, their variation in NMB throughout the day is significantly higher with a range from -0.25 to 0.25 across the average diurnal cycle. This approximately 2-fold difference in NMB variation due to implementing time-dependence describes the limits of the 'constant' and 'average' emissions scenarios is providing reliable simulated radon concentrations. Although the 'weekly' and 'daily'

scenarios do still exhibit some degree of bias, it consistently remains negative, making it much more predictable.

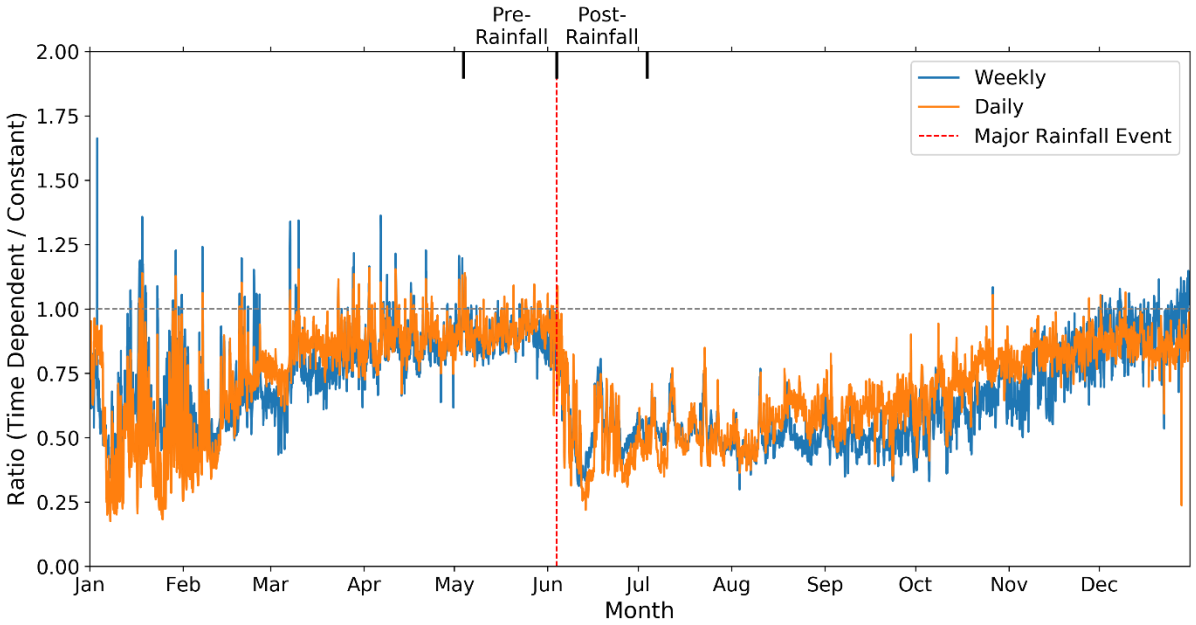

Figure 24: Time series for 2016 showing the ratio of radon concentrations from two time-dependent emissions scenarios (Weekly and Daily) to the constant radon emissions scenario.

When considering the differences in modelled radon performance between emissions scenarios, it is necessary to gain an understand of the temporal variations of the time-dependent 'daily' and 'weekly' scenarios, compared to the much simpler approach of using a constant value of radon emissions as in the 'constant' emissions scenario.

These differences are clearly visible in Figure 24 which uses the ratio of time-dependent to constant radon concentrations to visualise temporal differences. Generally, both time-dependent emissions scenarios have a similar relationship to constant emissions, with some slight variations throughout the year. In particular, the 'weekly' scenario exhibits a slower return to parity with the 'constant' emissions scenario, with the 'daily' scenario responding to drying conditions more rapidly. This is likely due to its increased complexity in relation to the daily scenario.

When examining the overall relationship between time-dependent and constant emissions, it is clear that the primary point of differences is seen during wet periods as seen following the Major rainfall event in Figure 24. The modelled concentrations during this period are almost half that of the

'constant' emissions scenario. Alternatively, periods of relatively low soil moisture (i.e. May 2016) produce modelled concentrations that are almost on par with 'constant' emissions, producing only slightly lower values on average.

A key point to consider from this trend is the sufficiency of using a constant radon emissions estimate during dry periods with very low soil moisture. During these time periods there is little improvement gained from incorporating the more complex, soil moisture driven models, which is also the case for climates with relatively low average rainfall. However, in this instance, due to the prevalence of rainfall in the Sydney Basin, these more complex models are highly necessary.

5.4.2. Major Rainfall Event

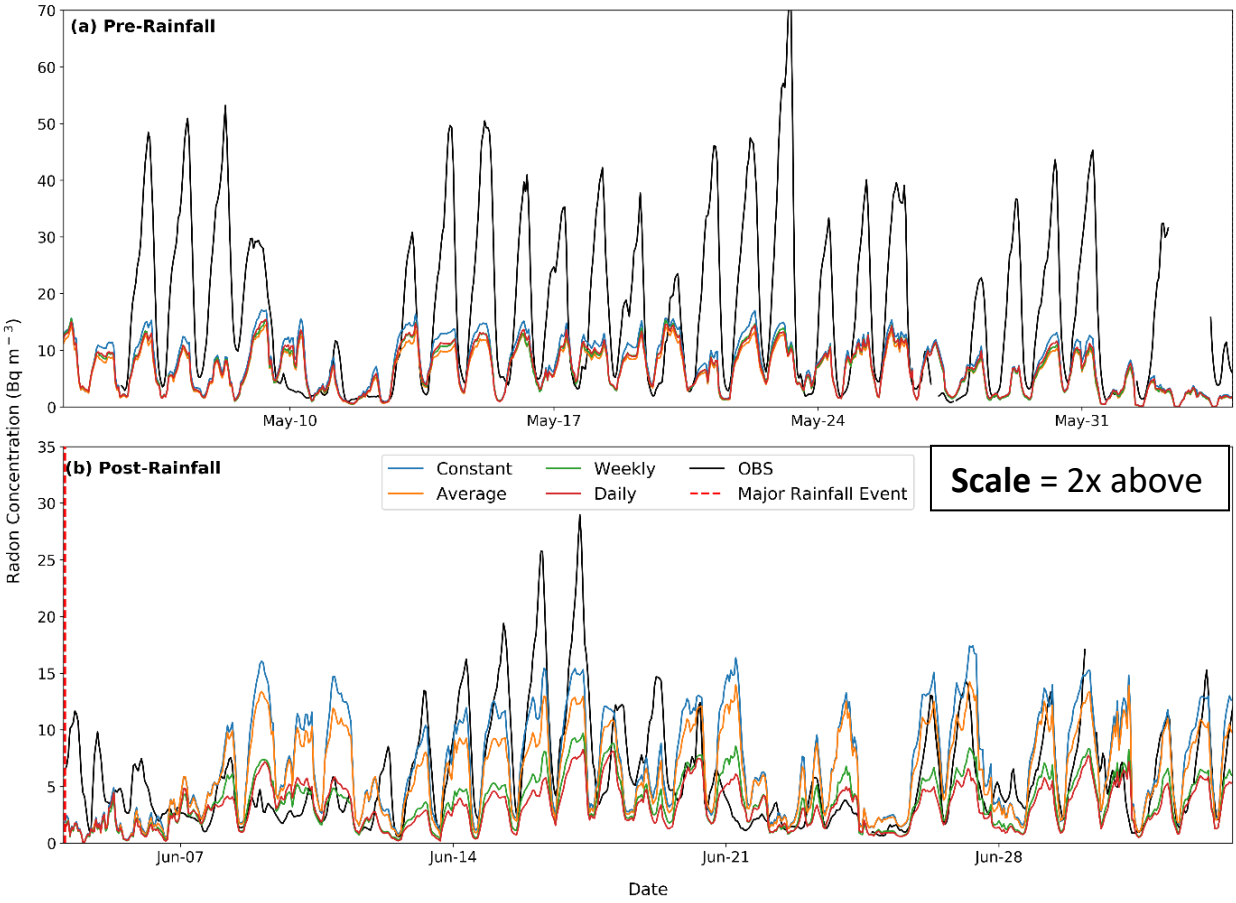

Figure 25: Timeseries of radon concentrations from observations and 4 emissions scenarios for 1 month before (a) Pre-Rainfall) and after (b) the June 4th major rainfall event.

For this study, one of the most effective methods of understanding this difference in model performance is comparing the response each model on a smaller timescale in relation to a major rainfall event. Examining modelled concentrations during a period of one month before ('Pre-rainfall') and after ('Post rainfall') this major rainfall event provides a clear picture of the response of each emissions scenario. The first trend that can be seen in Figure 25 is the large drop in maximum concentrations for observed radon concentrations following the rainfall event, in particular during the night-time. This response is mirrored by the 'weekly' and 'daily' scenario as their soil moisture component responds to the changes as a result of the rainfall. During the first week of the post-rainfall period these concentrations produce very similar results to the observed values. However, following this initial period of high correlation and as the soil begins to dry, observed radon concentrations return to having larger night-time spikes, which the time-dependent emissions scenarios fail to reflect.

Alternatively, both non-time dependent scenarios show little response to the major rainfall event with the night-time peaks only aligning closer to observed values after the initial saturation of the soil has subsided and the soil begins the dry.

These trends are repeated following a secondary rainfall event around the 20th of June (see Figure 15) after which the time-dependent emissions scenarios agree with observations initially but fail to maintain this once the initial saturation subsides. Figure 25 shows that in periods of extreme soil saturation, the 'weekly' and 'daily' scenarios perform very well as the nocturnal peaks in radon are supressed. However, this is short lived as the soil dries slightly and the nocturnal peaks return, at which point the correlation is weakened. As previously mentioned, this is driven by the poor performance of the model configuration in reflecting the nocturnal planetary boundary layer.

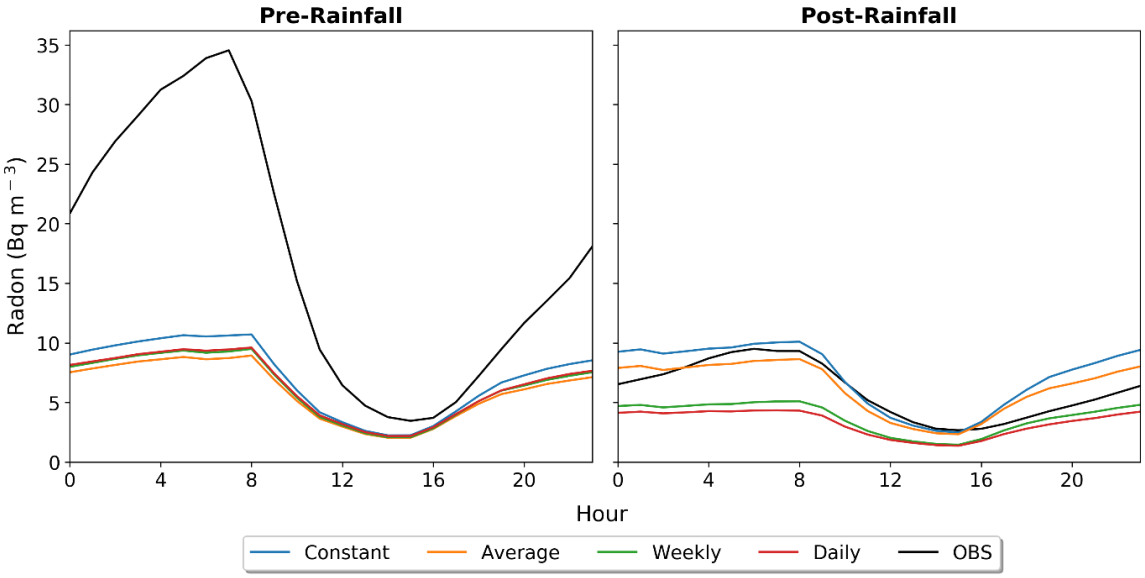

Figure 26: Mean diurnal cycle of radon concentrations from observations and 4 emissions scenarios for 1 month before (a) Pre-Rainfall) and after (b) the June 4th major rainfall event.

While these nocturnal peaks still remain following the major rainfall event, the magnitude is largely reduced (see Figure 26). It is only following this major rainfall event that the large diurnal cycle subdued, and night-time concentrations are somewhat reflected by the modelled radon concentrations. In this instance, the non-time dependent scenarios align more closely during these night-time hours.

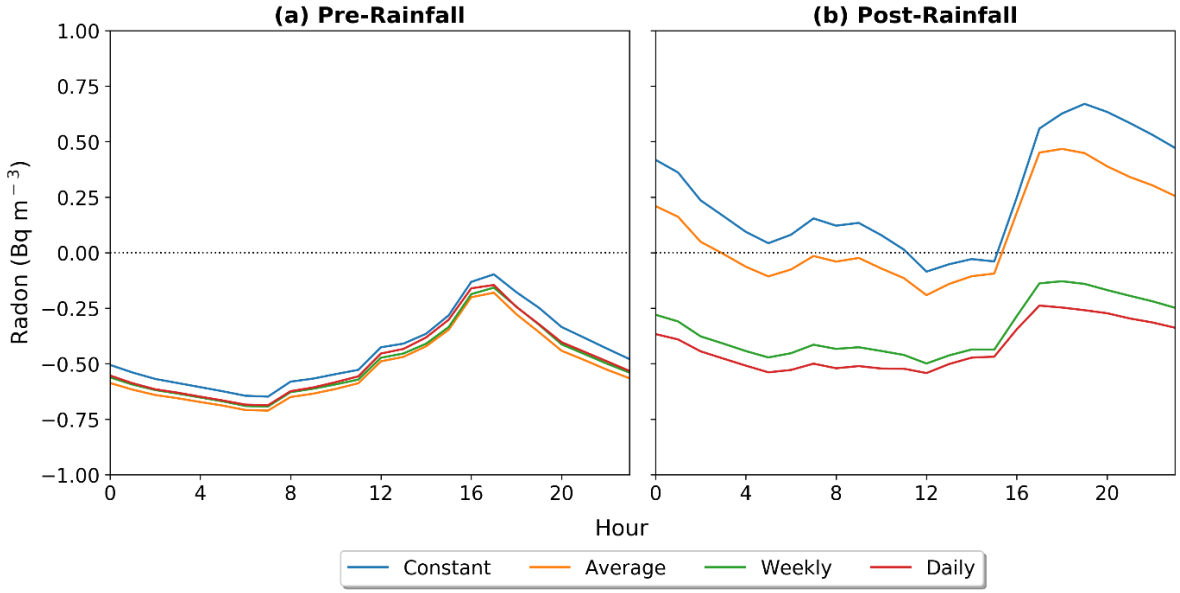

Figure 27: Diurnal cycle for normalised mean bias of radon concentrations from observations and 4 emissions scenarios for 1 month before (a) Pre-Rainfall) and after (b) the June 4th major rainfall event.

Figure 27 provides a very clear picture of the stark differences in response to rainfall events between the emissions scenarios, in particular what is driving the overall trends detailed earlier. As seen in Figure 23, when examining normalised mean bias of the different scenarios, there is an overall larger variation in normalised mean bias for the non-time dependent emissions scenarios compared to those driven by time-dependent soil moisture. During the abnormally dry 'Pre-rainfall' period, all emissions scenarios perform almost identically in relation to observed radon (see Figure 27a). This is even more so evident from examining the scatter plots of observed and modelled concentrations in which the 4 scenarios are almost indiscernible from each other (see Figure 28a). However, the overall NMB variation is still quite high at approximately 0.6, and night-time concentrations perform poorly with a -0.75 NMB, however day-time concentrations perform relatively well with a NMB up to -0.1. This shows the ability of the model to perform quite well during dry daytime conditions regardless of emissions scenario, despite poor performance at night.

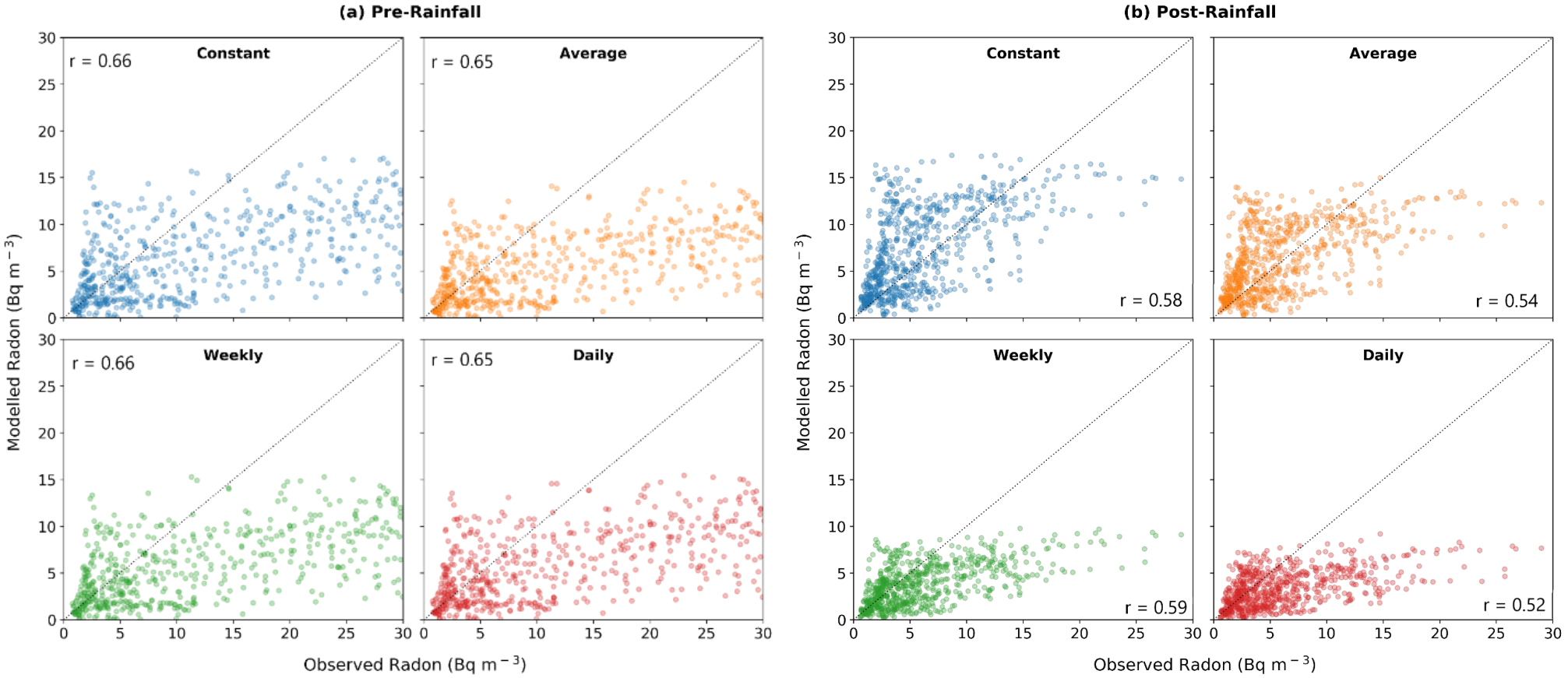

Figure 28: Scatter plots showing correlation of modelled radon and observed radon for 4 emissions scenarios for 1 month before (a) Pre-Rainfall) and after (b) the June 4th major rainfall event.

In response to the major rainfall event there is a clear divergence, as the ‘constant’ and ‘average’ scenarios see very little change (see Figure 26) , while the ‘weekly’ and ‘daily’ scenarios adjust to the change in soil moisture, but maintain a consistent normalised mean bias (Figure 27b).

In this instance these non-time dependent scenarios appear to be performing better post-rainfall than the others due to the NMB being close to 0 for much of the diurnal cycle. Despite this, the scatter plots for these scenarios (see Figure 28b) still show a relatively wide spread of values and a low correlations co-efficient (<0.6). The weekly and daily scenarios still exhibit a much more consistent and smaller variation in NMB (see Figure 27b), while also producing a relatively tight scatter plot spread post rainfall. It is likely that the non-time dependent emissions levels are somewhat representative of this post-rainfall situation, however this relatively good performance would be limited in its value across varying conditions.

Also, when comparing normalised mean bias of ‘Daily’ and ‘Weekly’ emissions scenarios, the ‘weekly’ scenario actually performs better during the post-rainfall period. Leading to the conclusion that there isn’t necessarily a clear improvement from adopting a newer, more complex soil moisture model.

In summary, the benefits of soil moisture driven, time-dependent emissions are still clear due to their ability to adapt consistently to changes in conditions, however their ability to estimate actual concentrations is primarily limited by model performance.

5.4.3. Seasonality

Seasonal variations in model performance produce some of the most drastic variations in radon concentrations and provide an idea of how each of the emissions scenarios perform across the full range of possible atmospheric conditions.

The most apparent change that is present between the seasons is the large variations in night-time observed radon concentrations as atmospheric conditions change and influence the stability and height of the nocturnal boundary layer. Autumn is the most extreme example of this with a mean radon concentration peak of approximately 25 Bq m^{-3} down to approximately 3 Bq m^{-3} at its low points. This peak is driven by more stable conditions leading to a shallower nocturnal boundary layer allowing for reduced vertical transport and thus higher concentrations. Alongside this large peak, Autumn exhibits very similar results across all emissions scenarios (see Figure 29). Overall, all other seasons exhibit much smaller nocturnal peaks, primarily due to increased stability. Across all seasons modelled radon concentrations remain relatively similar, with some divergence of time dependent and non-time dependent scenarios present during Winter and Spring.

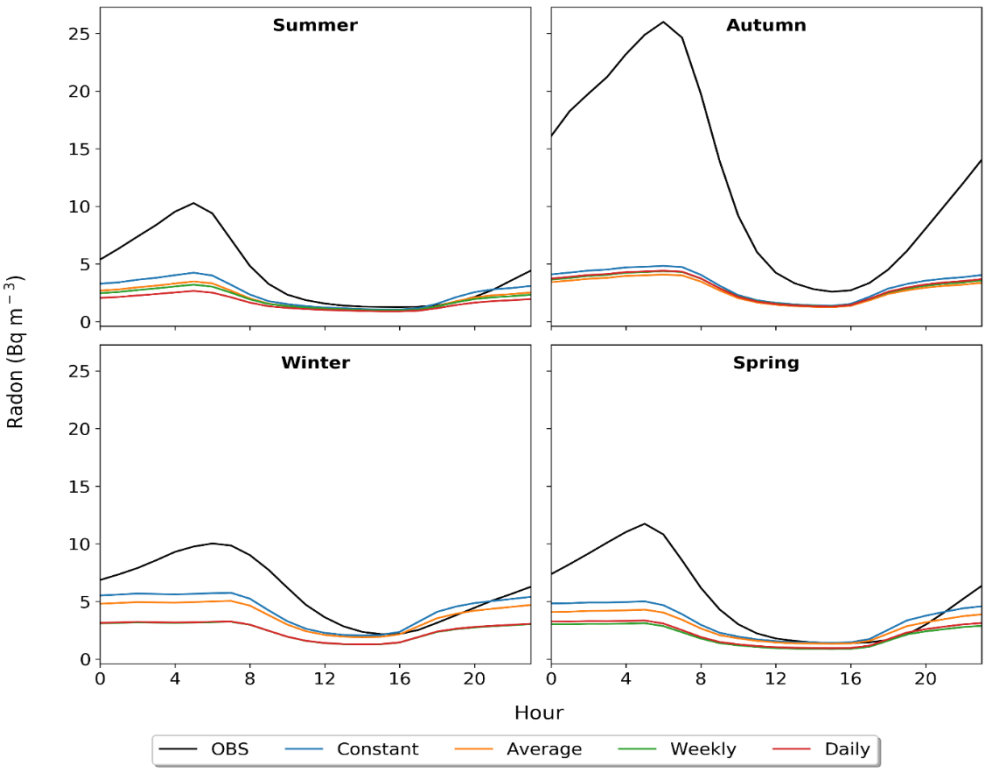

Figure 29: Mean diurnal cycle of radon concentrations from observations and 4 emissions scenarios for each season.

Figure 30 shows the agreement of each of the emissions scenarios across the 4 seasons. The difference between emission scenarios and their response to changed weather conditions is shown during winter as the time-dependent scenarios have a tighter spread of values, although it is still offset from the best fit. Generally, when the atmosphere is less stable the differences in emissions scenarios is more present as the bias is being driven less by high night-time concentrations.

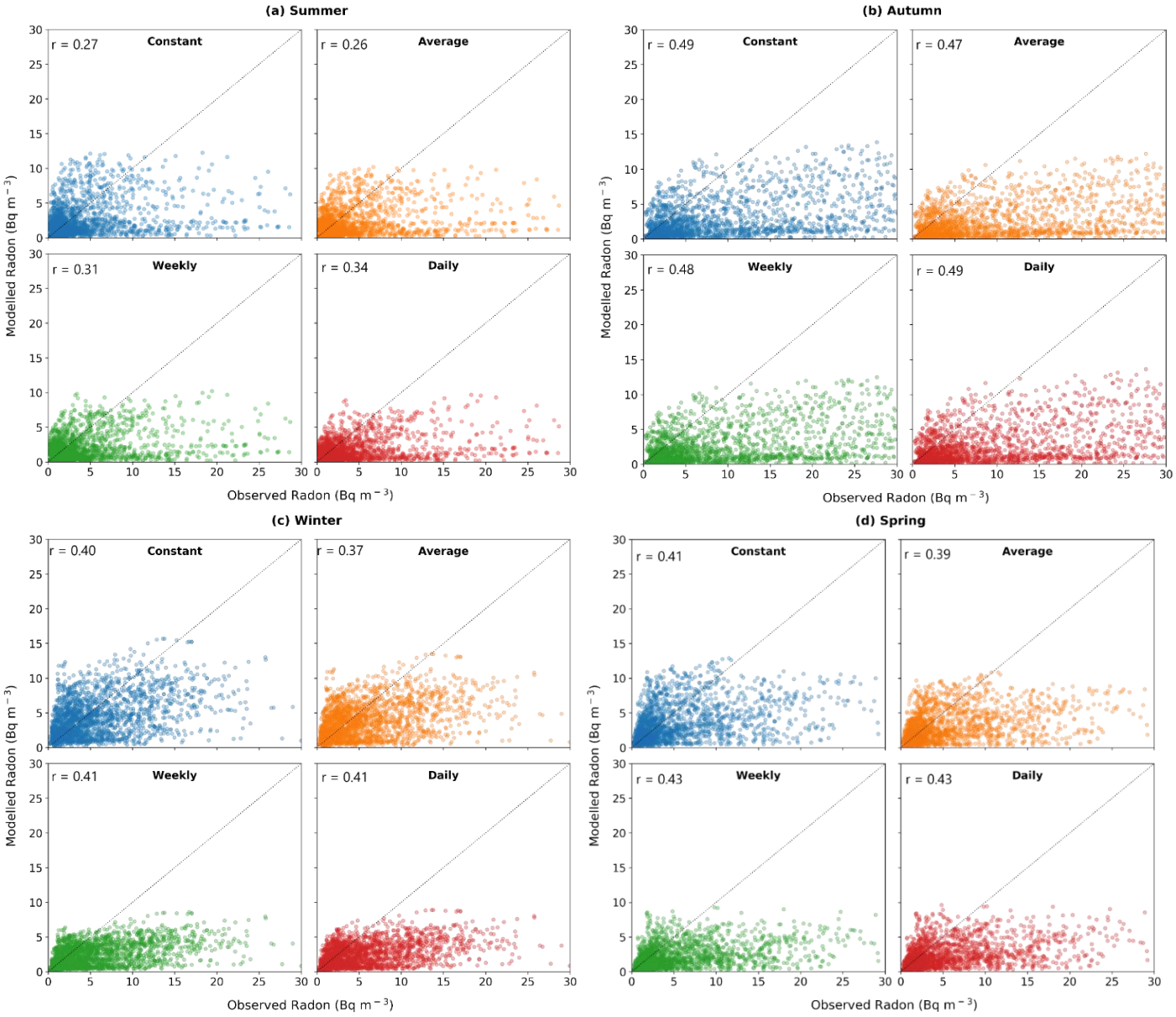

Figure 30: Scatter plots showing correlation of modelled radon and observed radon for 4 emissions scenarios for each season.

In summary, there are distinct seasonal trends present for radon, and as previously stated, effectively simulating this is difficult due to the large error of the model when simulating the planetary boundary layer.

6. Conclusion and Recommendations

6.1. Conclusions

This thesis aimed to gain an understanding of the role that soil moisture places in influencing modelled radon emissions in the Sydney Basin. In particular, examining trends and assessing the need for increased complexity of soil moisture parameters for emissions estimates. These goals were achieved by undertaking an analysis of a year's worth of data, in relation to a major rainfall event and assessing the response of each emissions scenario to these changes. From these aims, the following conclusions have been made:

- There is a clear link between changes in soil moisture and radon emissions, with an increase in soil moisture, leading to reduced radon emissions.

- There is a noticeable improvement in the accuracy and consistency of modelled radon concentrations when incorporating soil moisture into radon emissions estimates. This benefit is most noticeable during wet periods in which non-soil moisture driven scenarios fail to adapt to trends. Thus, implementing some degree of soil moisture input is beneficial.

- Increasing the complexity of the soil moisture input for emissions estimates appears to provide very little, if any, benefit to the performance of the radon model. Further, developments would likely see very little improvements over either of the currently available soil moisture models.

- It is clear that the most significant limitation driving model error currently is the poor performance of the model itself, rather than the soil moisture inputs. This is driven by the poor simulation of the nocturnal boundary layer by the model. This has led to poor estimates of radon concentrations for all emissions scenarios, which are currently a long way off accurately simulating radon.

These findings show the importance of understanding the driving factors behind atmospheric radon the need to understand its functioning on a deeper level in order to be able to focus future research

efforts more effectively. Further improvements in modelled radon will allow for effective simulations of key trace pollutants and develop our understanding of their functioning in our rapidly changing climate.

6.2. Recommendations for future work

Future research into radon emissions and the role of soil moisture in influencing their function should primarily focus on the improvement of the atmospheric transport models used in an attempt to bring modelled concentrations in line with observed radon values.

This field would also benefit from the analysis various different model parameters and their relationship to model performance in order to determine further limiting factors of simulating radon-222.

The radon time-series used may also have been affected by the slow response time of the radon detector used, thus deconvolution may provide some improvement across all simulations (Griffiths et al., 2016).

References

Appleton, J. D. 2007, 'Radon: Sources, Health Risks, and Hazard Mapping', *British Geological Survey*, vol. 36, no. 1, pp. 85-9.

Arya, S. P. 1999, *Air pollution meteorology and dispersion*, vol. 6, Oxford University Press New York.

Ayotte, J., Flanagan, S. & Morrow, W. 2007, *Occurrence of Uranium and 222 Radon in Glacial and Bedrock Aquifers in the Northern United States, 1993-2003 Scientific Investigations Report 2007-5037*.

Balsamo, G., Albergel, C., Beljaars, A., Boussetta, S., Brun, E., Cloke, H., Dee, D., Dutra, E., Muñoz-Sabater, J., Pappenberger, F., De Rosnay, P., Stockdale, T. & Vitart, F. 2015, 'ERA-Interim/Land: a global land surface reanalysis data set', vol. 19, no. 1, pp. 389-407.

Biraud, S., Ciais, P., Ramonet, M., Simmonds, P., Kazan, V., Monfray, P., O'Doherty, S., Spain, T. G. & Jennings, S. G. 2000, 'European greenhouse gas emissions estimated from continuous atmospheric measurements and radon 222 at Mace Head, Ireland', *Journal of Geophysical Research: Atmospheres*, vol. 105, no. D1, pp. 1351-66.

BOM 2019a, *Richmond RAAF - 2016 Daily Rainfall Data*, Australian Bureau of Meterology, viewed 1/10/2019, <http://www.bom.gov.au/jsp/ncc/cdio/weatherData/av?p_nccObsCode=136&p_display_type=dailyDataFile&p_startYear=2016&p_c=-900749609&p_stn_num=067105>.

—— 2019b, *Richmond RAAF - Monthly Rainfall Data*, Australian Bureau of Meterology, viewed 1/10/2019, <http://www.bom.gov.au/jsp/ncc/cdio/weatherData/av?p_nccObsCode=139&p_display_type=dataFile&p_startYear=&p_c=&p_stn_num=067105>.

Chambers, S., Williams, A., Crawford, J. & Griffiths, A. 2015, 'On the use of radon for quantifying the effects of atmospheric stability on urban emissions', *Atmospheric Chemistry and Physics*

vol. 15, no. 3, pp. 1175-90.

Chambers, S., Williams, A. G., Zahorowski, W., Griffiths, A. & Crawford, J. 2011, 'Separating remote fetch and local mixing influences on vertical radon measurements in the lower atmosphere', *Tellus B: Chemical and Physical Meteorology*, vol. 63, no. 5, pp. 843-59.

Chambers, S. D., Guérette, E.-A., Monk, K., Griffiths, A. D., Zhang, Y., Duc, H., Cope, M., Emmerson, K. M., Chang, L. T., Silver, J. D., Utembe, S., Crawford, J., Williams, A. G. & Keywood, M. 2019, 'Skill-Testing Chemical Transport Models across Contrasting Atmospheric Mixing States Using Radon-222', *Atmosphere*, vol. 10, no. 1, p. 25.

Chambers, S. D., Williams, A. G., Conen, F., Griffiths, A. D., Reimann, S., Steinbacher, M., Krummel, P. B., Steele, L. P., Van Der Schoot, M. V., Galbally, I. E., Molloy, S. B. & Barnes, J. E. 2016, 'Towards a Universal "Baseline" Characterisation of Air Masses for High- and Low-Altitude Observing Stations Using Radon-222', *Aerosol and Air Quality Research*, vol. 16, no. 3, pp. 885-99.

Cope, M., Keywood, M., Emmerson, K., Galbally, I., Boast, K., Chambers, S., M, C., Crumeyrolle, S., Dunne, E., Fedele, R., Gillett, R., Griffiths, A., Harnwell, J., Katzfey, J., Hess, D., Lawson, S. J., Miljevic, B., Molloy, S., Powell, J. & Zeng, J. 2014, *The Sydney Particle Study*, The Centre for Australian Weather and Climate Research.

Crawford, J., Chambers, S., Cohen, D., Williams, A., Griffiths, A. & Stelcer, E. 2016, 'Assessing the impact of atmospheric stability on locally and remotely sourced aerosols at Richmond, Australia, using Radon-222', *Atmospheric Environment*, vol. 127, pp. 107-17.

Field, W. R., Krewski, D., Lubin, J. H., Zielinski, J. M., Alavanja, M., Catalan, V. S., Klotz, J. B., Létourneau, E. G., Lynch, C. F., Lyon, J. L., Sandler, D. P., Schoenberg, J. B., Steck, D. J., Stolwijk, J. A., Weinberg, C. & Wilcox, H. B. 2006, 'An Overview of the North American Residential Radon and Lung Cancer Case-Control Studies', *Journal of Toxicology and Environmental Health: Part A Current Issues*, vol. 69, no. 7-8, pp. 599-631.

Frost, A. J., Ramchurn, A., Smith, A. 2018, *The Australian Landscape Water Balance model (AWRA-L v6). Technical Description of the Australian Water Resources Assessment Landscape model version 6.*, Bureau of Meteorology.

Greater Sydney Commission 2018, *Greater Sydney Region Plan - A Metropolis of Three Cities*, NSW Government.

Griffiths, A. D., Chambers, S. D., Williams, A. G. & Werczynski, S. 2016, 'Increasing the accuracy and temporal resolution of two-filter radon–222 measurements by correcting for the instrument response', *Atmos. Meas. Tech.*, vol. 9, no. 6, pp. 2689-707.

Griffiths, A. D., Parkes, S. D., Chambers, S. D., McCabe, M. F. & Williams, A. G. 2013, 'Improved mixing height monitoring through a combination of lidar and radon measurements', *Atmospheric Measurement Techniques*, vol. 6, no. 2, pp. 207-18.

Griffiths, A. D., Zahorowski, W., Element, A. & Werczynski, S. 2010, 'A map of radon flux at the Australian land surface', *Atmospheric Chemistry and Physics*, vol. 10, no. 18, pp. 8969-82.

Gupta, M. L., Douglass, A. R., Kawa, S. R. & Pawson, S. 2004, 'Use of radon for evaluation of atmospheric transport models: sensitivity to emissions', *Tellus B: Chemical and Physical Meteorology*, vol. 56, no. 5.

Hart, M., De Dear, R. & Hyde, R. 2006, 'A synoptic climatology of tropospheric ozone episodes in Sydney, Australia', vol. 26, no. 12, pp. 1635-49.

Hirsch, A. 2007, 'On using radon-222 and CO 2 to calculate regional-scale CO 2 fluxes', *Journal of Atmospheric Chemistry & Physics*

vol. 7, no. 14, pp. 3737-47.

Holford, D. J., Schery, S. D., Wilson, J. L. & Phillips, F. M. 1993, 'Modeling radon transport in dry, cracked soil', *Journal of Geophysical Research-Solid Earth*, vol. 98, no. B1, pp. 567-80.

Horsley, J. A., Broome, R. A., Johnston, F. H., Cope, M. & Morgan, G. G. 2018, 'Health burden associated with fire smoke in Sydney, 2001-2013', *Medical Journal of Australia*, vol. 208, no. 7, pp. 309-10.

Ishimori, Y., Lange, K., Martin, P., Mayya, Y. S. & Phaneuf, M. 2013, *Measurement and Calculation of Radon Releases from NORM Residues*, INTERNATIONAL ATOMIC ENERGY AGENCY, Vienna.

Jacob, D. J. & Prather, M. J. 1990, 'Radon-222 as a test of convective transport in a general circulation model', *Tellus B: Chemical and Physical Meteorology*, vol. 42, no. 1.

Jacob, D. J., Prather, M. J., Rasch, P. J., Shia, R.-L., Balkanski, Y. J., Beagley, S. R., Bergmann, D. J., Blackshear, W. T., Brown, M., Chiba, M., Chipperfield, M. P., De Grandpré, J., Dignon, J. E., Feichter, J., Genthon, C., Grose, W. L., Kasibhatla, P. S., Köhler, I., Kritz, M. A., Law, K., Penner, J. E., Ramonet, M., Reeves, C. E., Rotman, D. A., Stockwell, D. Z., Van Velthoven, P. F. J., Verver, G., Wild, O., Yang, H. & Zimmermann, P. 1997, 'Evaluation and intercomparison of global atmospheric transport models using 222 Rn and other short-lived tracers', *Journal of Geophysical Research*, vol. 102, no. D5, pp. 5953-70.

Jin, Y. & Jury, W. A. 1996, 'Characterizing the dependence of gas diffusion coefficient on soil properties', *Soil Science Society of America Journal*, vol. 60, no. 1, pp. 66-71.

Kalwarf, D. R., Nielson, K. K., Rich, D. C. & Rogers, V. C. 1982, *Comparison of radon diffusion coefficients measured by transient-diffusion and steady-state laboratory methods*, NUREG/CR-2875; PNL-4370; RAE-18-3; Other: ON: DE83004556 United States 10.2172/6872243 Other: ON: DE83004556 NTIS, PC A03/MF A01 - GPO PNNL English, Rogers and Associates Engineering Corp., Salt Lake City, UT (USA).

Karstens, U., Schwingshackl, C., Schmithüsen, D. & Levin, I. 2015, 'A process-based 222 radon flux map for Europe and its comparison to long-term observations', *Atmospheric Chemistry and Physics*, vol. 15, no. 22, pp. 12845-65.

Kirkham, M. B. 2014, *Principles of soil and plant water relations*, Academic Press.

Millington, R. J. & Quirk, J. P. 1960, 'Transport in Porous Media', *Proceedings of the 7th International Congress of Soil Science, Madison, Wisconsin, USA*, vol. 1, pp. 97-106.

Moldrup, P., Olesen, T., Yoshikawa, S., Komatsu, T. & Rolston, D. 2004, 'Three-Porosity Model for Predicting the Gas Diffusion Coefficient in Undisturbed Soil', *Soil Science Society of America Journal*, vol. 68.

Monk, K., Guérette, E.-A., Paton-Walsh, C., Silver, J. D., Emmerson, K. M., Utembe, S. R., Zhang, Y., Griffiths, A. D., Chang, L. T. C., Duc, H. N., Trieu, T., Scorgie, Y. & Cope, M. E. 2019, 'Evaluation of Regional Air Quality Models over Sydney and Australia: Part 1—Meteorological Model Comparison', *Atmosphere*, vol. 10, no. 7, p. 374.

National Research Council 1999, *Health Effects of Exposure to Radon: BEIR VI*, The National Academies Press, Washington, DC.

Nazaroff, W. W. 1992, 'Radon transport from soil to air', *Reviews of geophysics*, vol. 30, no. 2, pp. 137-60.

Nazaroff, W. W. & Nero, A. V. 1988, 'Radon and its decay products in indoor air'.

Nielson, K. K., Rogers, V. C., Rich, D. C., Nederhand, F. A., Sandquist, G. M. & Jensen, C. M. 1981, *Laboratory measurements of radon diffusion through multilayered cover systems for uranium tailings*, PNL-4107; UMT-0206; Other: ON: DE82006072; TRN: 82-015707 United States 10.2172/5361667 Other: ON: DE82006072; TRN: 82-015707 NTIS, PC A07/MF A01. PNNL English, ; Rogers and Associates Engineering Corp., Salt Lake City, UT (USA).

NSW-EPA 2012, *Air emissions inventory for the greater metropolitan region in New South Wales. 2008 Calendar Year*, NSW-Environment Protection Authority: Sydney, Australia.

Porstendörfer, J. 1994, 'Properties and behaviour of radon and thoron and their decay products in the air', *Journal of Aerosol Science*, vol. 25, no. 2, pp. 219-63.

Prospero, J. M. & Carlson, T. N. 1970, 'Radon-222 in the North Atlantic trade winds: Its relationship to dust transport from Africa', *Science*, vol. 167, no. 3920, pp. 974-7.

Raupach, M., Briggs, P., Haverd, V., King, E., Paget, M. & Trudinger, C. 2009, *Australian water availability project (AWAP): CSIRO marine and atmospheric research component: final report for phase 3*, CSIRO Marine and Atmospheric Research.

Rodell, M., Houser, P. R., Jambor, U., Gottschalck, J., Mitchell, K., Meng, C. J., Arsenault, K., Cosgrove, B., Radakovich, J., Bosilovich, M., Entin, J. K., Walker, J. P., Lohmann, D. & Toll, D. 2004, 'The Global Land Data Assimilation System', *Bulletin of the American Meteorological Society*, vol. 85, no. 3, pp. 381-94.

Rogers, V. C. & Nielson, K. K. 1991, 'Correlations for predicting air permeabilities and 222Rn diffusion coefficients of soils', *Health physics*, vol. 61, no. 2, pp. 225-30.

Schery, S. D. & Wasiolek, M. A. 1998, *Modeling radon flux from the earth's surface*, World Scientific Publishing Co Pte Ltd, Singapore.

Sesana, L., Barbieri, L., Facchini, U. & Marcazzan, G. 1998, '222Radon as a tracer of atmospheric motions: a study in Milan', *Journal of Radiation Protection Dosimetry*, vol. 78, no. 1, pp. 65-72.

Skamarock, W. C., Klemp, J., Dudhia, J., Gill, D. O., Barker, D. & Wang, W. 2008, 'A Description of the Advanced Research WRF Version 3', *NCAR Tech. Note*, vol. 27, pp. 3-27.

Sportisse, B. 2009, *Fundamentals in air pollution: from processes to modelling*, Springer Science & Business Media.

Stockwell, D. Z. & Chipperfield, M. P. 1999, 'A tropospheric chemical-transport model: Development and validation of the model transport schemes', *Quarterly Journal of the Royal Meteorological Society*, vol. 125, no. 557, pp. 1747-83.

Taylor, S. A. 1949, 'Oxygen diffusion in porous media as a measure of soil aeration', *Proceedings. Soil Science Society of America, 1949*, vol. 14, pp. 55-61.

Vogeltanz-Holm, N. & Schwartz, G. G. 2018, 'Radon and lung cancer: What does the public really know?', *Journal of Environmental Radioactivity*, vol. 192, pp. 26-31.

Vogiannis, E. G. & Nikolopoulos, D. 2015, 'Radon Sources and Associated Risk in Terms of Exposure and Dose', *Frontiers in Public Health*, vol. 2.

Whittlestone, S. & Zahorowski, W. 1998, 'Baseline radon detectors for shipboard use: Development and deployment in the First Aerosol Characterization Experiment (ACE 1)', *J. Geophys. Res.*, vol. 103, no. D13, pp. 16743-51.

Wigand, A. & Wenk, F. 1928, 'Der Gehalt der Luft an Radium-Emanation, nach Messungen bei Flugzeugaufstiegen', vol. 391, no. 13, pp. 657-86.

Williams, A. G., Chambers, S. D., Conen, F., Reimann, S., Hill, M., Griffiths, A. D. & Crawford, J. 2016, 'Radon as a tracer of atmospheric influences on traffic-related air pollution in a small inland city', *Tellus B: Chemical and Physical Meteorology*, vol. 68, no. 1, p. 30967.

Yoon, J. Y., Lee, J.-D., Joo, S. W. & Kang, D. R. 2016, 'Indoor radon exposure and lung cancer: a review of ecological studies', *Annals of occupational and environmental medicine*, vol. 28, pp. 15-.

Zahorowski, W., Chambers, S. D. & Henderson-Sellers, A. 2004, 'Ground based radon-222 observations and their application to atmospheric studies', *Journal of Environmental Radioactivity*, vol. 76, no. 1, pp. 3-33.

Zhang, K., Feichter, J., Kazil, J., Wan, H., Zhuo, W., Griffiths, A. D., Sartorius, H., Zahorowski, W., Ramonet, M., Schmidt, M., Yver, C., Neubert, R. E. M. & Brunke, E. G. 2011, 'Radon activity in the lower troposphere and its impact on ionization rate: a global estimate using different radon emissions', *Atmos. Chem. Phys.*, vol. 11, no. 15, pp. 7817-38.

Zhuo, W., Guo, Q., Chen, B. & Cheng, G. 2008, 'Estimating the amount and distribution of radon flux density from the soil surface in China', vol. 99, no. 7, pp. 1143-8.

Zhuo, W., Iida, T. & Furukawa, M. 2006, 'Modeling Radon Flux Density from the Earth's Surface', vol. 43, no. 4, pp. 479-82.